UNIVERSITY OF MINNESOTA
ST. ANTHONY FALLS HYDRAULIC LABORATORY

Project Report No. 134

A Preliminary Report on the Zero-Crossing-Rate Technique for Average Shear Measurement in Flowing Fluid

by
JOSEPH M. WETZEL
and
JOHN M. KILLEN

This research was sponsored by the Naval Ship Systems Command General Hydromechanics Research Program administered by the Naval Ship Research and Development Center under Contracts N00014-67-A-0113-0007 and N00014-67-A-0113-0015.

NOVEMBER 1972
MINNEAPOLIS, MINNESOTA

CONTENTS

LIST OF ILLUSTRATIONS

PREFACE

This is a final report under Contract N00014-67-A-0113-0007 and a supplementary report under Contract N00014-67-A-0113-0015 in that most of the studies in the 4-inch pipe facility were carried out under the second contract number.

A March 1968 proposal called for the measurement of surface pressure fluctuations and wall shear fluctuations. Measurements were to include shear intensity spectra, correlation measurements of surface shear fluctuations and surface pressure fluctuations, and space correlation of surface shear fluctuations.

The work was begun after October 1968 under the first-referenced contract and continued until April 1970 under a no-cost extension.

Measurements were made of surface pressure fluctuation intensity spectra on smooth and rough surfaces with the addition of drag reducing polymer and were reported in St. Anthony Falls Hydraulic Laboratory Project Report No. 119 [6]. Shear fluctuation measurements will be covered in the present report. Instrumentation difficulties were encountered with the correlation measurements, and time and funds were exhausted before any meaningful results were obtained.

---

*Numbers in brackets refer to list of references on pages 14-15.

ABSTRACT

The characteristics of a flush-mounted hot film sensor were investigated in turbulent flows of both water and drag reducing polymer solutions in a 4-inch-diameter pipe. For water flows, a linear relationship was found between the average power supplied to the sensor and the cube root of the wall shear stress. With the addition of polymer additives, the heat transfer rates at a given shear stress were reduced from those found with water alone. Analysis of the heat transfer fluctuations occurring in various flow facilities has shown that the zero crossing rate is related to the wall shear stress and to fluid properties for water, polymer, and air flows. The zero crossing rate is not dependent on hot film sensitivity or contamination. Evaluations of the fluctuation microscale indicated that it had been increased by the addition of drag reducing polymer to the water. Autocorrelation measurements were made of the heat transfer fluctuations, but the limited data for the autocorrelations were not conclusive. Attempts to obtain cross-correlation coefficients between heat transfer and surface pressure fluctuations as measured with a small hydrophone were unsuccessful. The zero crossing rate of the surface pressure fluctuations was found to be related to the local wall shear stress.

A PRELIMINARY REPORT ON THE ZERO-CROSSING-RATE TECHNIQUE FOR AVERAGE SHEAR MEASUREMENT IN FLOWING FLUIDS

I. INTRODUCTION

A number of fundamental studies of dilute polymer flows conducted at the St. Anthony Falls Hydraulic Laboratory have required that a measurement be made of the average local wall shear stress. A flush-mounted hot film sensor has been employed for this purpose. Calibration of the sensor indicated that the power supplied to the sensor was proportional to the cube root of the average wall shear stress for turbulent water flow [1,2]*. However, the addition of even very small quantities of drag reducing polymer to the flow resulted in a change in the calibration curve similar to the changes noted with hot film sensors used for velocity measurements [3]. This discouraging finding led to an investigation of alternative techniques and eventually to examination of the fluctuating component of heat transfer. Armistead and Keyes [4] have reported some measurements with a flush-mounted hot film sensor of the zero crossing rate of the heat transfer fluctuations for water flow in a pipe and have shown that the zero crossing rate is linearly proportional to the pipe Reynolds number. Preliminary measurements with a similar probe at the St. Anthony Falls Hydraulic Laboratory have shown that the zero crossing rate can also be related to the two-thirds power of the average wall shear stress for water flowing in a pipe. The data were very reproducible, and the increased sensitivity to shear stress using the fluctuations rather than average values of output voltage provided incentive for the development of an instrument or technique using zero crossing rate as a measure of local shear stress at a boundary. Preliminary results of this technique for various flow environments are described in the sections that follow. A number of the findings require further verification, and the studies are being continued under support from the National Science Foundation.

---

*Numbers in brackets refer to list of references on pages 14-15.

II. EXPERIMENTAL APPARATUS

A. Experimental Facilities

Three experimental facilities were used in the preliminary investigation: a gravity-flow water pipe facility [5], a rotating cylinder [6], and an air pipe facility through which air was drawn by a centrifugal blower [7].

1. Gravity-Flow Water Pipe Facility

A schematic layout of the gravity-flow pipe facility is shown in Fig. 1. Fifty feet of 4-in.-diameter pipe were laid horizontally, with the test section located 114 diameters downstream of the beginning of the straight reach. Untreated water was drawn directly from the Mississippi River and was discharged to waste under a 50 ft head. Discharge was controlled by the gate valves and was measured with a calibrated metering elbow. A flow straightener consisting of 3/4-in. tubes about 1.5 ft long was placed at the pipe entrance to reduce the effects of the upstream elbow. Four 1/8-in.-diameter piezometer taps were carefully drilled and deburred at each of the locations shown. Pressure drops used in the calculation of wall shear stress were measured over each of the distances shown as well as over the entire test reach of 10 ft. Preliminary tests indicated that the pressure gradient was constant and the flow was fully developed at the test section.

Aqueous solutions of polyethylene oxide WSR-301 with concentrations of 250 and 500 ppm by weight were mixed in a large storage tank located at a higher level in the laboratory. Gentle agitation was used in the mixing. A low head pump was used to transfer the polymer from the tank to the pipe, and the polymer was injected at the low pressure side of the upstream elbow as shown in Fig. 1. The injection rate was determined by measuring the change in fluid level in the calibrated storage tank for a given period of time. The concentration of the homogeneous polymer solution in the test section was calculated from the known injected and pipe discharges.

The polymer solutions were analyzed for drag reducing properties with a capillary tube blowdown rheometer. A sample withdrawn from the pipe at the test section was checked against a sample collected from the storage tank and diluted to the proper concentration. The results agreed satisfactorily, indicating that complete mixing had taken place and that degradation effects were minor.

2. Rotating Cylinder Test Facility

This facility has been described previously in Ref. [6]. Pertinent parts of the description are repeated here for convenience. A sketch of this facility is shown in Fig. 2. The rotating cylinder was positioned on the axis of a steel tank 6 ft in diameter and 6 ft high. The tank was supported on three I-beams. A cork pad was installed between the I-beams and the concrete floor of the laboratory for sound isolation. Sandbags were placed against the exterior walls of the tank to provide additional damping of the tank wall as well as some isolation from sound transmitted through the air.

The tank capacity was 1260 gallons. It was filled to a 5-1/2-ft depth from the municipal water supply or from the St. Anthony Falls Hydraulic Laboratory's 6-in. water tunnel. The water tunnel is also filled from the municipal water supply; however, it is equipped with an air separator and pressure control and thus provides a simple and rapid means of removing dissolved and free air from the water to the concentration level required. Diversion of water from the water tunnel to the tank enabled tests to be conducted with various dissolved air contents. A steam heat exchanger was also installed in the tank to permit adjustment or control of the water temperature.

The rotating cylinder was supported on a hollow stainless steel shaft mounted in water-lubricated rubber bearings. The cylinder itself was 1 ft long with an external diameter of 1 ft. Its top was submerged 2 ft below the static water surface in the tank. The cylinder was hollow to provide space for instruments and was constructed of a synthetic wood material (Renwood) with brass end plates 1/4 in. thick. Renwood cones were attached to both end plates. A wall thickness of 3 in. was selected to reduce cylinder wall vibrations. This type of construction has proved to be free of any detectable resonant peak in the noise spectrum. The cylinder and end cones were finished with a heavy coat of epoxy paint. The surface was machined to a 0.001 in. "runout," dynamically balanced, and polished to a high gloss. It was waxed frequently during the test program to assure that it approached a hydraulically smooth surface.

The cylinder shaft was supported by a wood framework attached to the laboratory floor and wall, avoiding contact with the tank. A water-lubricated rubber bearing and thrust washer connected the cylinder, drive shaft, and pulleys to the support frame. A second rubber guide bearing mounted on a cross frame inside the tank was necessary to hold the cylinder in an axial position. The cross frame also supported a 2-ft-diameter disk immediately above the cylinder to prevent air from being drawn down the vortex core which was present in the tank during operation. The cylinder was driven by a 20 hp, 3500 rpm induction motor through a "V" belt drive. Speed changes were effected by various combinations of pulleys on the motor and cylinder shaft.

A set of strain gages was mounted on the drive shaft of the rotating cylinder and served to measure the total torque exerted by the fluid on the cylinder and end cones. A second dynamometer was mounted in one of the end cones to measure the drag on the cone separately so that the total torque could be corrected for end effects. The corrected torque was used to calculate the average shear stress on the cylinder surface.

3. Air Pipe Test Facility

A complete description of this facility is given in Ref. [7], and an overall sketch is shown in Fig. 3. The pipe was a transparent cast acrylic tube with a 3-inch inside diameter made up of eight 48-inch lengths, one 24-inch length, and two 6-inch lengths accurately coupled at each joint. Air from the room was drawn through the pipe into the suction line of a large blower. The flow rate was measured with a calibrated orifice plate near the downstream end of the test section.

Four piezometer holes of 1/16-in. diameter were located at the pipe quadrants 3 in. from the downstream end of each 48-in. pipe length. They were drilled in a milling machine to insure that they were exactly perpendicular to the pipe wall. The holes were carefully deburred to a 1/64-in. radius using a specially made tool and jig, after which they were inspected with the aid of a magnifying glass. The four holes were connected to a manifold to reduce dependence on one hole and thereby increase the reliability of the measurements.

Pressure drops were measured in the test reach, which extended from 33 to 137 pipe diameters from the inlet. Fully developed flow was found to exist in the test reach. The hot film sensor was installed 96 pipe diameters from the inlet.

B. Instrumentation

The hot film sensor used in all tests was a Model No. 1236W flush-mounted quartz-coated unit obtained from Thermo-Systems, Inc. The sensor was attached to a traversing mechanism to permit movement in the radial direction as well as rotation about its own longitudinal axis. Radial position with respect to the pipe wall was measured with an Ames dial reading to within 0.001 in., and the rotation was measured with a protractor accurate to one degree. The sensor was connected to a Thermo-Systems, Inc., Model 1020A anemometer. The cold resistance of the sensor was measured before and after each test run and was found to be very stable. An overheat ratio of 10 per cent was used in tests involving water or polymer flows; higher overheat ratios were employed with air flows.

The output of the anemometer was fed into various electronic devices for further processing. Average bridge output voltage was measured with a Weston digital voltmeter modified to give a 10-second integrating time. The rms voltage of the fluctuating signal was measured with a Disa Random Signal Indicator and Correlator, Type 55A06. Frequency analysis was carried out with a Hewlett-Packard 300H harmonic wave analyzer having an 11 Hz effective bandwidth. The signal from the anemometer was also fed into a voltage comparator circuit which delivered a pulse when a reference voltage was sensed. Electrical noise of small amplitude made it necessary to set the comparator to sense a small positive voltage. The number of positive going pulses was counted with a Hewlett-Packard electronic counter. A 10-second count of the zero crossings was made to give a good average.

III. RESULTS

A. Sensor Calibration

The hot film sensor was mounted in the water pipe facility at the probe location shown in Fig. 1. Prior to the attempt to obtain a calibration curve for the sensor as a function of average wall shear stress, considerable effort was expended to determine the influence of the orientation of the sensor with respect to the pipe wall and the direction of flow. To this end the position of the sensor face along the pipe radius was varied. The element orientation was varied by rotation of the sensor itself. The most useful signals were obtained when the heated element was placed so that the smallest dimension was parallel to the flow. For the radial position studies the entire sensor was moved systematically so that the face of the sensor was projected either into the flow or into the pipe wall and the corresponding average bridge voltage and the rms of the fluctuating component of the bridge voltage were measured. These tests were conducted for various velocities in water flow only. A typical plot is shown in Fig. 4 for an average velocity of 13.6 fps. A small range of radial positions existed for which the bridge voltage was essentially constant and the rms voltage was at a minimum. The width of this region was dependent on velocity, decreasing as the velocity increased. This small radial range of position of the sensor included the flush position as determined visually and by touch. Therefore, for all succeeding tests the radial position of the sensor was located by visual inspection at the flush position.

The calibration curve obtained in the water pipe facility is shown in Fig. 5 plotted as the average bridge output voltage squared against the cube root of the average wall shear stress. The wall shear stress was calculated from the measured pressure drop. The open symbols represent data for water and the filled symbols data taken with polymer injection. For water flow, an essentially linear relationship is noted between the plotted parameters. As the concentration of Polyox was increased, the average shear stress and bridge voltage were reduced, but not in accordance with the relationship obtained with water. At a given shear stress the bridge voltage, and thus the heat transfer, was less for the polymer solution than for water.

In most cases the data were obtained by selecting a particular shear stress for an initial water flow rate and then gradually increasing the polymer injection rate. As a result of friction reduction, the flow rate and average velocity increased slightly. Thus the Reynolds number also increased slightly for each particular set of data. Some of the tests were conducted with the concentration of polymer held constant. The calibration curve so obtained is shown in Fig. 6 for a polymer concentration of 10 ppm. The same data have been plotted in Fig. 7 to show the magnitude of drag reduction and changes in the average bridge voltage squared as a function of Reynolds number. Drag reduction at a given Reynolds number was calculated as the difference in the friction factor for water and polymer flows divided by the friction factor for water. The values of ΔE_B^2 were also calculated by taking the difference in E_B^2 for water and polymer flows and dividing by the value for water flow only. However, as the bridge voltage decreases with decreasing shear stress, the value of bridge voltage for water flow was taken at the same shear stress as for the polymer flow at any given Reynolds number. Thus ΔE_B^2 indicates the influence of the polymer addition on the average output of the hot film sensor.

B. Zero Crossing Rate - Heat Transfer Fluctuations

The first measurements of the positive-going zero crossing rate of the heat transfer fluctuations were made in the 4-inch pipe with water flow to serve as a basis of comparison with the experiments reported by Armistead and Keyes [4]. Data taken and analyzed as described above and plotted versus Reynolds number are shown in Fig. 8. By taking the data at different times of the year, it was possible to obtain a variation of viscosity through temperature of the river water. The data at a given temperature are linearly related to the Reynolds number; however, the curves for different temperatures are displaced. At a given Reynolds number the zero crossing rate is higher for low water temperatures. It is thus assumed that the experiments of Armistead and Keyes [4] were conducted at a constant fluid temperature and that the Reynolds number was changed only by varying the velocity. The linear relationship found by Armistead and Keyes is shown by the broken line. Their data were limited to Reynolds numbers less than 1.68×10^5.

To further substantiate these findings, similar measurements were made in the rotating cylinder facility, where the fluid temperature was more readily variable. The results are shown in Fig. 9, in which ω is the rotational speed and a is the radius of the cylinder. The same general trends with water temperature and Reynolds were noted. Also plotted are some data taken for a homogeneous 50 ppm solution of Polyox WSR-301. The kinematic viscosity for water was used in calculating the Reynolds number. The data vary linearly with the Reynolds number with a further reduction in zero crossing rate as compared to the data for water at essentially the same temperature.

In an effort to find a group of variables which would result in an improved correlation of the data, it was assumed that the zero crossing rate of the heat transfer fluctuations was an indication of the breakdown rate of the viscous sublayer. Einstein and Li [8] have proposed the following relationship:

$$\bar{\tau}_o = \frac{2U_o \, \varrho \nu^{1/2}}{\sqrt{\pi} \, T^{1/2}}$$

in which $\bar{\tau}_o$ = average local shear stress

ϱ = fluid density

ν = kinematic viscosity

U_o = velocity at the edge of the sublayer

T = average time for sublayer to grow to an unstable value

In the current work, an undefined length L is introduced and U_o is written as L/T. The number of zero crossings per unit time, N_o, is taken as $1/T$. It is thus possible to rewrite the above equation as

$$N_o \propto \frac{(\bar{\tau}_o)^{2/3}}{\varrho^{2/3} \, \nu^{1/3} \, L^{2/3}}$$

As the fluid density appears in this relationship, it was of interest to vary the density over a wide range. Thus, experiments were also conducted using air as the flowing fluid.

The experimental data obtained from the previously described facilities and reduced to the above form are plotted in Fig. 10. The length L has been chosen as unity under the assumption that it is a constant or at most a slowly changing function of the flow parameters. A great improvement in the data correlation is noted even for the case in which a drag reducing polymer has been added to the water.

It should also be mentioned that early in the test program one of the hot film sensors was destroyed. The calibration curve for the replacement was different from that of the first sensor. However, in repeating some of the test runs with the new sensor, it was found that the data for the zero crossing rate as a function of average shear stress agreed with the previous results. Some of the data taken with the first sensor are shown in Fig. 10 with flagged symbols. Thus it appears that the fluctuating component of the heat transfer is not sensitive to the calibration of the sensor, and perhaps a calibration curve is not even required. If this possibility is verified by the additional studies currently being carried out in another investigation, the technique may prove to be very useful in measuring average local wall shear stress.

The above speculations have considered only a single dimension in the viscous sublayer. It has been shown by Kline, et al. [10] that the viscous sublayer is three-dimensional. Further experimental evidence given by Meek [11] as to the ratios of the various length scales indicates that the flow-wise length of sublayer spots (correlated regions) is nearly 60 times the spanwise length. Drag reduction by polymer addition seems to act through a modification of the sublayer. The shift in the velocity profile, as noted by Meyer [12], is an indication of increased sublayer thickness and of flow modification in this region.

The flow mechanism involved in the observed phenomena of zero crossing rate correlation with average shear is known only in a vague manner from general knowledge of sublayer behavior. Black [13] has suggested that pressure fluctuations as measured with a surface-mounted pressure transducer should also be a measure of average wall shear.

C. Frequency Spectra

Frequency spectra of the heat transfer fluctuations were taken for nearly all test runs with the hot film probe in both water and polymer flows. Typical trends of the data are shown in Fig. 11 for the power spectral density $F(n)$ on a dB scale as a function of the frequency. The power spectra have been normalized with the mean square voltage integrated over the frequency range of the spectra. The total rms is reduced by increasing the concentration of polymer as indicated in the legend. The higher frequencies, above about 100 Hz, are also attenuated by the addition of polymer.

The power spectra, corrected for bandwidth of the analyzer, have been plotted in dimensionless form in Fig. 12 using the pipe diameter, D, and the average velocity V as reference quantities. The spectra for water (open symbols) collapse very well except at the higher frequencies, where some discrepancies are observed. The same trend exists for the polymer data (filled symbols) at the higher frequencies.

Using the calibration curve shown in Fig. 5 for water flow, the fluctuating component of the bridge voltage was converted into a fluctuating component of wall shear, ϕ, at a given frequency. A dimensionless plot of the fluctuating shear as a function of frequency is shown in Fig. 13 for two sets of data taken with water and different values of the average wall shear stress. The data for the two tests compare very well at the higher frequencies, with deviations being noted at the lower frequencies. This is exactly the opposite of the trend that is observed in the plot of Fig. 12. Experimental data for polymer flows have not been reduced in this form due to the anomalies in the calibration curves.

D. Microscale

Assuming a Gaussian distribution and isotropic turbulence, the microscale, λ, can be determined for a turbulent fluctuation by any of several methods [14]. Although it was realized that the assumed conditions of a Gaussian distribution might not be satisfied at the boundary, it was of interest to compare the values of the microscale with and without polymers.

If $u(t)$ is the turbulent fluctuation, then

$$\frac{1}{\lambda^2} = \frac{1}{U^2 \overline{u^2}} \overline{\left(\frac{\partial u}{\partial t}\right)^2} = \frac{4\pi^2}{U^2} \int_0^\infty n^2 F(n)\, dn = \frac{4N_o^2 \pi^2}{U^2}$$

Thus the microscale can be found from the derivative of $u(t)$, from the second moment of the power spectra, and from the number of positive-going zero crossings in $u(t)$.

Values of the microscale obtained by the latter two methods as a function of polymer concentration for an essentially constant Reynolds number are shown in Fig. 14. The velocity, U, was taken as the average velocity in the pipe. As the polymer concentration was increased, the microscale also increased, and it appears that a maximum occurs at a concentration of about 20 ppm, which corresponds roughly to the concentration required for maximum drag reduction.

As a further check on the consistency of the measurements of the frequency spectra and zero count, data were compared for a wide range of conditions. A plot of the square root of the integral in the above equation versus the number of positive-going zero crossings is shown in Fig. 15. The data points for both water and polymer flows tend to scatter about the solid line, indicating satisfactory agreement between the two methods.

In the plots of $n^2F(n)$ versus n a maximum value of $n^2F(n)$ was observed. A typical plot using the spectral data in Fig. 11 is shown in Fig. 16. The frequency at which the maximum occurs is a measure of the frequency of the eddies that provide the major contribution to the total dissipation. Data for a number of experiments conducted in the 4-inch pipe facility with both water and polymer flows are shown in Fig. 17. In Fig. 17a the frequency at which the maximum occurred is plotted as a function of percentage of drag reduction. Different symbols were used in plotting only to distinguish data obtained for a given test run. Considerable scatter of data is noted, but a definite trend can be observed. As the drag reduction due to polymer injection increases, the maximum of the $n^2F(n)$ curve occurs at lower frequencies. These data can be reduced in terms of a wave number through division by the convective velocity. The convective velocity was not known in this case, and therefore the average flow velocity was used to convert the frequencies to the wave number, k_d. Results are shown in Fig. 17b. This plotting tended to reduce the scatter of the data for the flows with drag reduction, but a considerable number of discrepancies are still noted for water flow alone. From these results it appears that the effect of polymer additive is to increase the size of the turbulent eddies at which maximum dissipation occurs. Further experiments are being carried out to more completely verify these findings.

E. Autocorrelation Measurements

Autocorrelation coefficient measurements were made of the fluctuating signal from the hot film probe mounted on the surface of the rotating cylinder. A Disa Correlator Model 55A06 was used in conjunction with an Ad-YU Model 802F delay line to obtain a correlation coefficient.

Results for a smooth cylinder surface are shown in Figs. 18 and 19 for water only and for 10 ppmw Polyox 301 dissolved in the test water. Data taken with no polymer additive showed the typical exponential decrease of the correlation coefficient; however, the correlation times appear unusually long unless considered in the light of the very low velocity in the surface layer.

The addition of polymer seems to bring about some marked differences; however, due to the limited amount of data, this result should be viewed with caution.

F. Zero Crossing Measurements - Surface Pressure Fluctuations

Measurements were made of the zero crossing rate of the fluctuating output signal from a 1/8-inch-diameter surface pressure hydrophone. The hydrophone was mounted flush with the smooth surface of the rotating cylinder. Figure 20 shows the results as plotted against average shear stress to the two-thirds power. The data for various concentrations of polymer all fall along a single line. Little difference in drag was observed for this range of polymer concentrations. The drag with water alone was about twice that with various concentrations of polymer. The shift in relative position on various runs depends at present on the adjustment of the frequency response and sensitivity and should not be regarded as significant; only the slope of the line is significant. The difference between the slope for the data taken in polymer solutions and that for the data taken in water in Fig. 20 possibly has some flow-related significance.

IV. CONCLUSIONS

1. A calibration of a flush-mounted hot film sensor has been carried out in a 4-in. pipe facility. For water flow the square of the average bridge voltage was a linear function of the cube root of the average wall shear stress. For flows of homogeneous solutions of Polyox WSR-301 the heat transfer from the sensor at a given shear stress level was reduced from that found in water flows.

2. The number of zero crossings of the heat transfer fluctuations was linearly related to the Reynolds number. However, varying the liquid viscosity through temperature resulted in a different linear relationship. Data for the zero crossing rate for a wide range of flow conditions and fluid properties were shown to be correlated with the breakdown rate of the viscous sublayer proposed by Einstein and Li [8]. As the zero crossing rate was proportional to the average local shear stress, the technique may prove useful in measurements of wall shear stress for many applications. Further studies are being carried out to verify the preliminary findings.

3. Measurements of the frequency spectra indicated that the polymer additive attenuated the high-frequency portion of the spectra. The microscale determined from the second moment of the frequency

spectra, $n^2F(n)$, and also from the number of zero crossings was larger for polymer flows than for water. The frequency at which the maximum of the $n^2F(n)$ curve occurred was found to decrease with increasing drag reduction, indicating a shift to a larger size of the turbulent eddies associated with maximum dissipation.

4. Limited measurements of the autocorrelation coefficient of the heat transfer fluctuation in the rotating cylinder facility with water indicated a typical exponential decrease. The delay times appeared to be unusually long. Some differences were noted for the polymer solution; however, the limited data were not conclusive. Attempts to obtain a cross-correlation between heat transfer and surface pressure fluctuations were plagued with instrumentation difficulties and were thus unsuccessful.

5. The zero crossing rate of surface pressure fluctuations as measured with a small flush-mounted hydrophone on a smooth rotating cylinder was a linear function of the average shear stress to the two-thirds power. However, the slope of the line through the data points was greater for polymer solutions than for water alone. Surface pressure fluctuations could not be measured in the pipe facilities due to low flow velocities and excessive background noise.

REFERENCES

[1] Bellhouse, B. J. and Schultz, D. L., "Determination of Mean and Dynamic Skin Friction Separation and Transition in Low-Speed Flow with a Thin-Film Heated Element," Journal of Fluid Mechanics, Vol. 24, Pt. 2, 1966, pp. 379-400.

[2] Liepmann, H. W. and Skinner, G. T., "Shearing Stress Measurements by Use of a Heated Element," TN 3268, NACA, 1954.

[3] Friehe, C. A. and Schwartz, W. H., "Static Tubes and Hot Film Anemometers in Dilute Polymer Solutions," Viscous Drag Reduction, C. S. Wells, Ed., Plenum Press, 1969.

[4] Armistead, R. A. and Keyes, J. J., "A Study of Wall-Turbulence Phenomena Using Hot Film Sensors," Journal of Heat Transfer, ASME, February 1968, pp. 13-21.

[5] Wetzel, J. M.; Almo, J. A.; and Killen, J. M., "Turbulence Measurements in Dilute Polymer Flows," Turbulence Measurements in Liquids, proceedings of Symposium on Turbulence Measurements in Liquids, Univ. of Missouri, Rolla, September 1969, G. K. Patterson and J. L. Zakin, Eds., pp. 96-101.

[6] Killen, J. M., The Influence of Drag Reducing Polymers on Surface Pressure Fluctuations on Rough Surfaces, Project Report No. 119, St. Anthony Falls Hydraulic Laboratory, University of Minnesota, September 1971.

[7] Blaisdell, F. W. and Hebaus, G. C., Hydraulics of Closed Conduit Spillways - Part XI. Tests Using Air, Technical Paper No. 44-B, St. Anthony Falls Hydraulic Laboratory, University of Minnesota, January 1966.

[8] Einstein, H. A. and Li, H., "The Viscous Sublayer along a Smooth Boundary," Proceedings, ASCE, Paper 945, EM Vol. 82, No. 2, April 1956, pp. 1-27.

[9] van Driest, E. R., "Turbulence Drag Reduction of Polymeric Solutions," Journal of Hydronautics, July 1970, pp. 120-126.

[10] Kline, S. J.; Reynold, W. C.; Schraub, F. A.; and Runstadler, R. W., "The Structure of Turbulent Boundary Layers," Journal of Fluid Mechanics, Vol. 30, Pt. 4, 1967, pp. 741-773.

[11] Meek, R. L., "A Study of the Viscous Sublayer in Turbulent Flow," Ph.D. Thesis, University of Utah, 1968.

[12] Meyer, W. A., "A Correlation of the Frictional Characteristics for Turbulent Flow of Dilute Non-Newtonian Fluid in Pipes," AIChE Journal, 12, 1966, pp. 522-525.

[13] Black, T., "Some Practical Applications of a New Theory of Wall Turbulence," Heat and Mass Transfer Institute, Santa Clara, 1966.

[14] Liepmann, H. W.; Laufer, J.; and Leipmann, K., "On the Spectrum of Isotropic Turbulence," TN 2473, NACA, 1951.

I L L U S T R A T I O N S

(Figures 1 through 20)

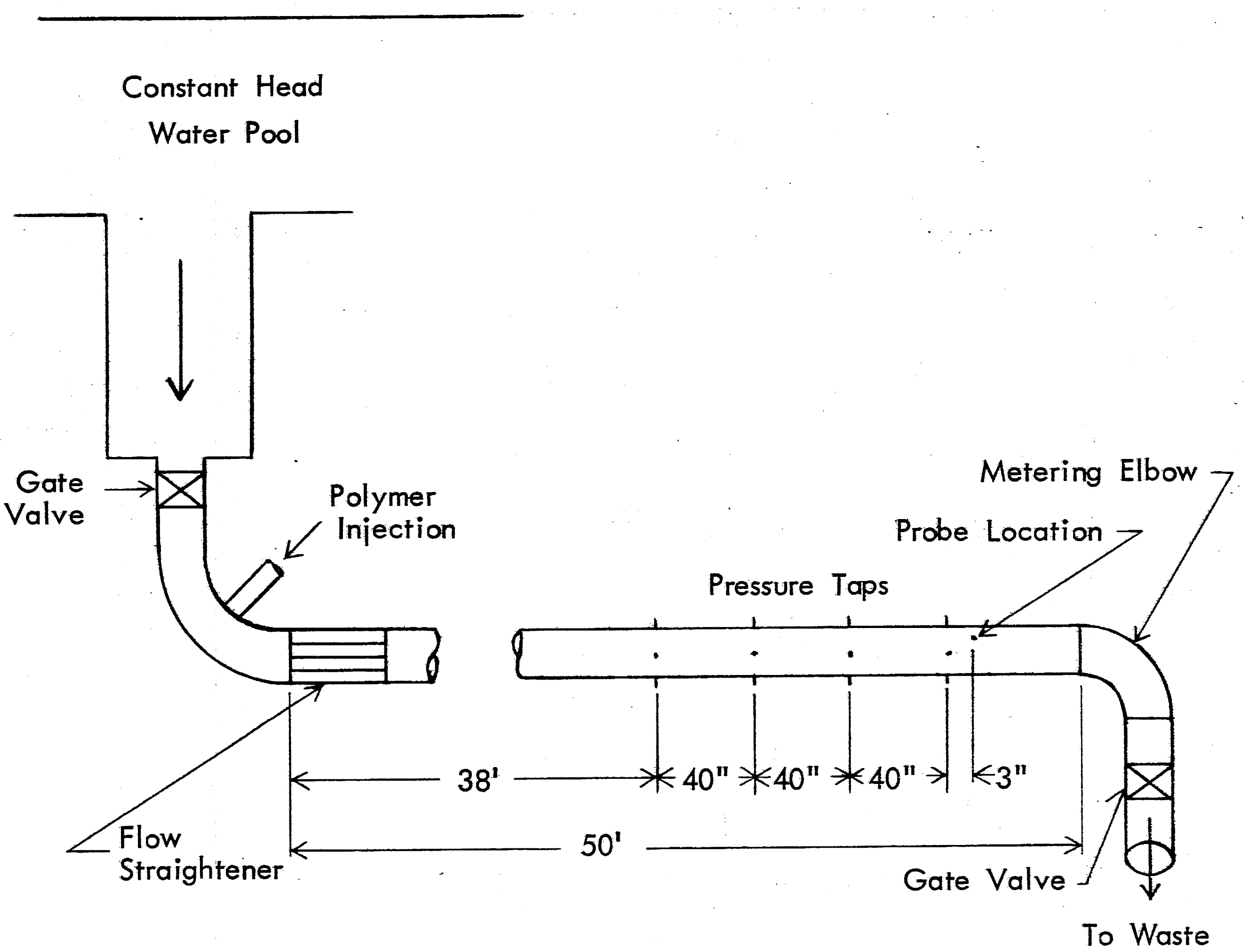

Fig. 1 - Four-Inch Pipe Gravity Flow Facility

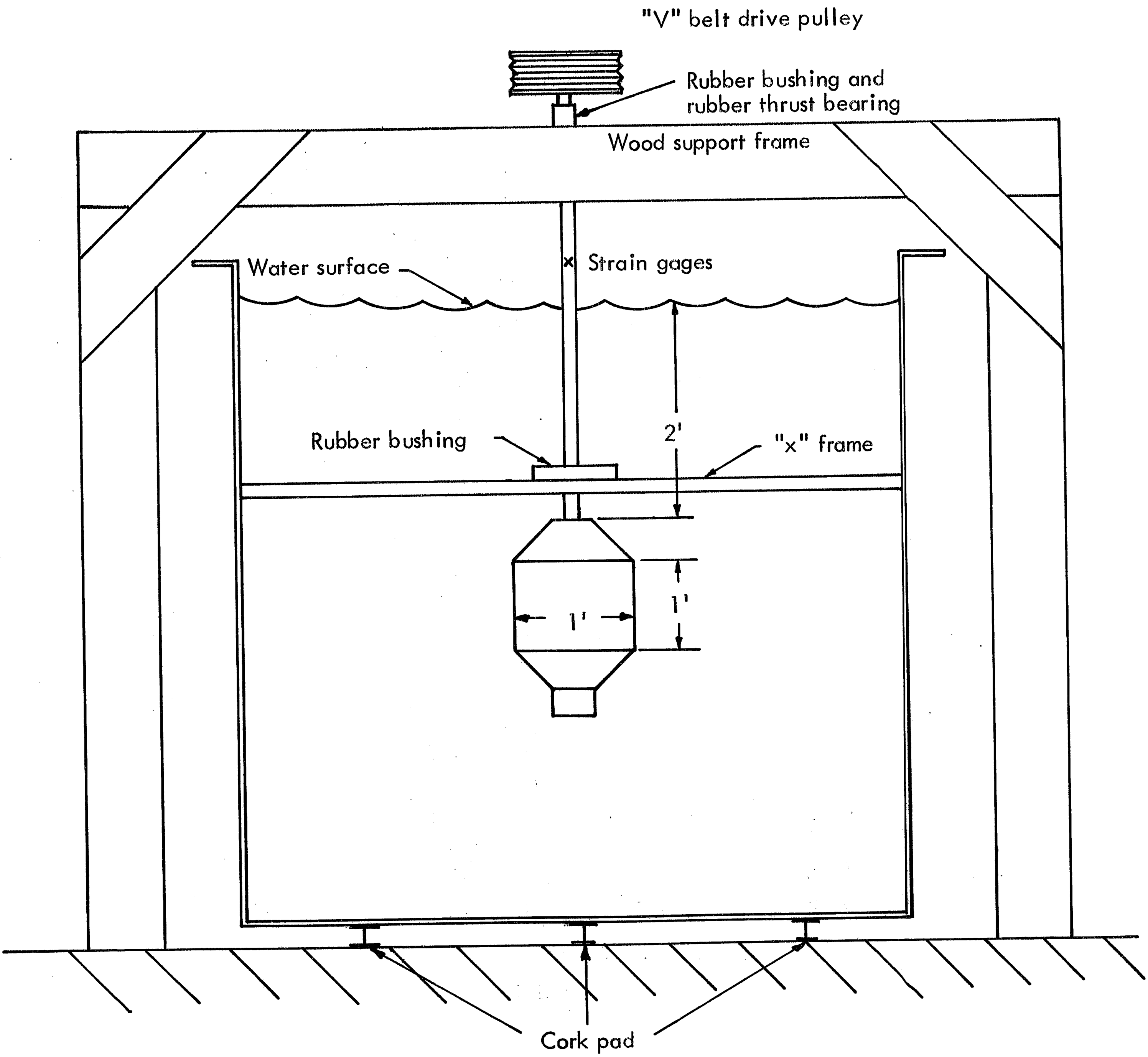

Fig. 2 - Rotating Cylinder Facility

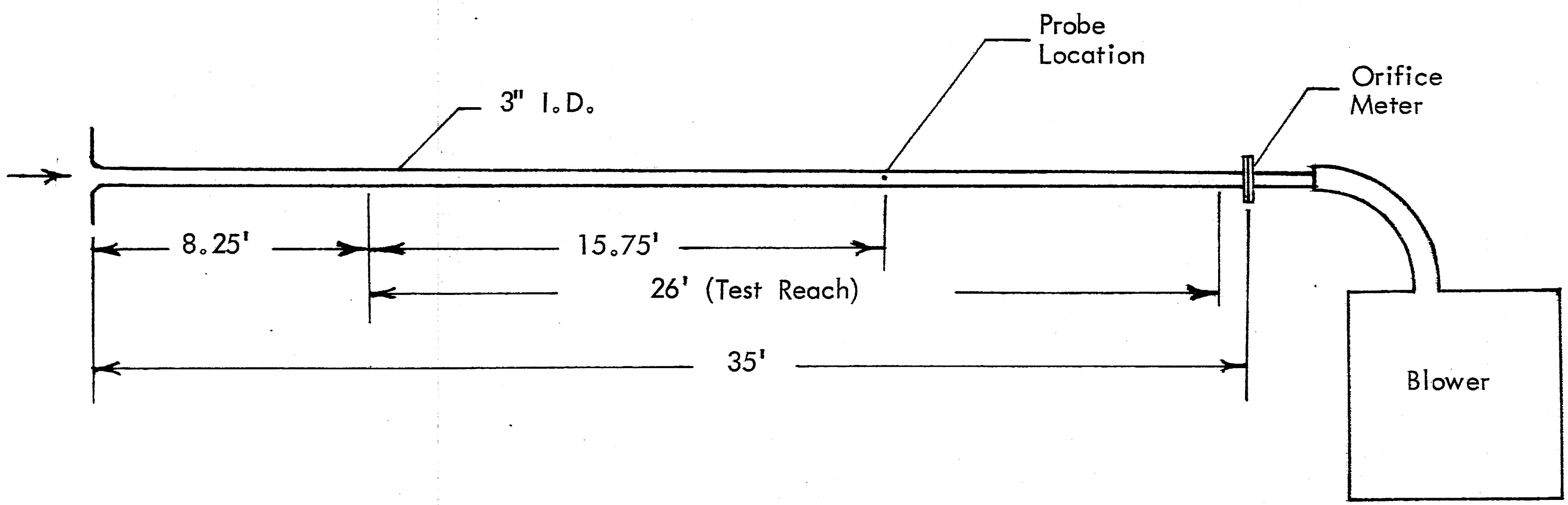

Fig. 3 - Three-Inch Air Pipe Facility

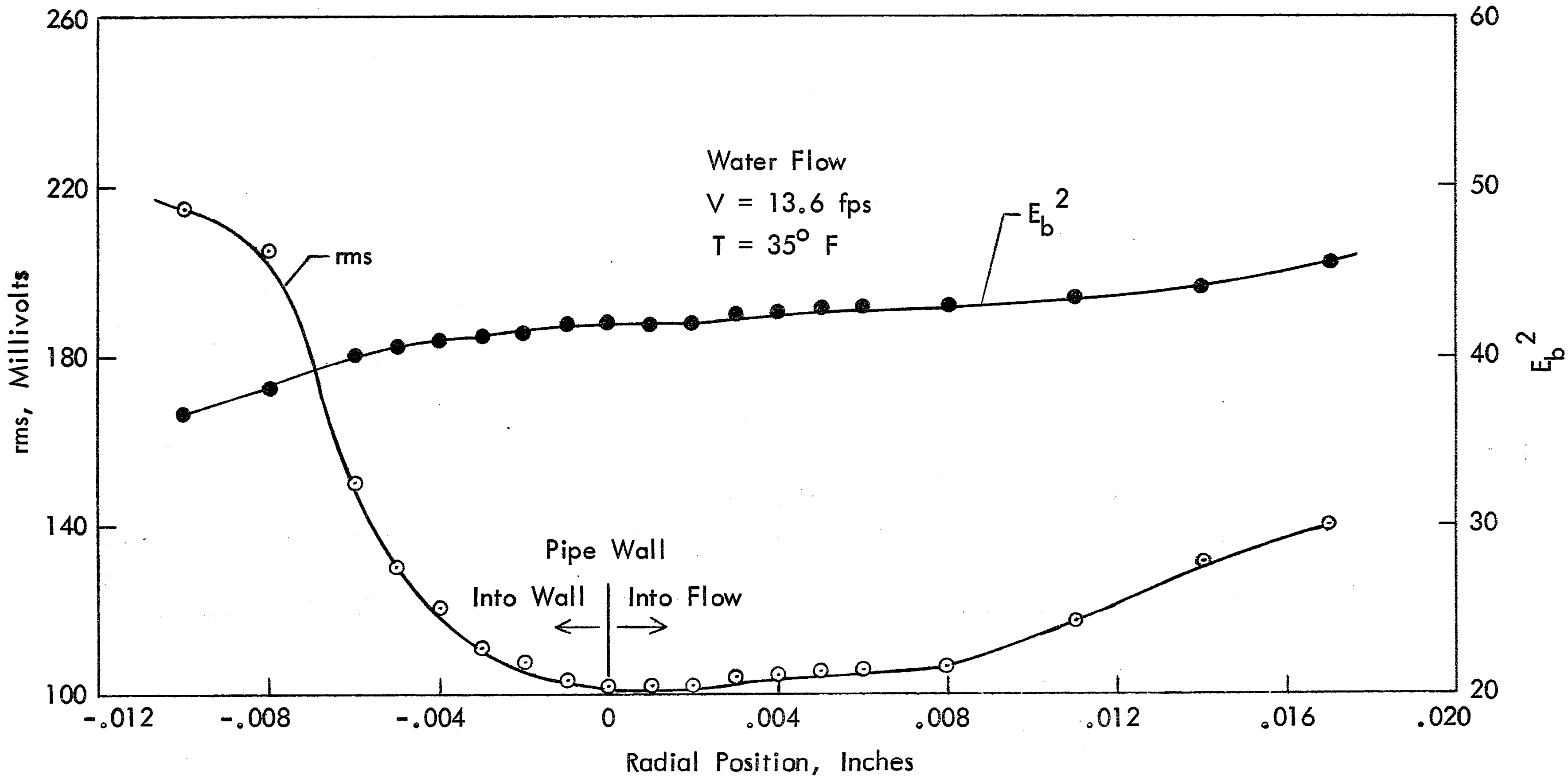

Fig. 4 - Effect of Varying Radial Position of Hot Film Sensor with respect to Boundary, 4 Inch Pipe

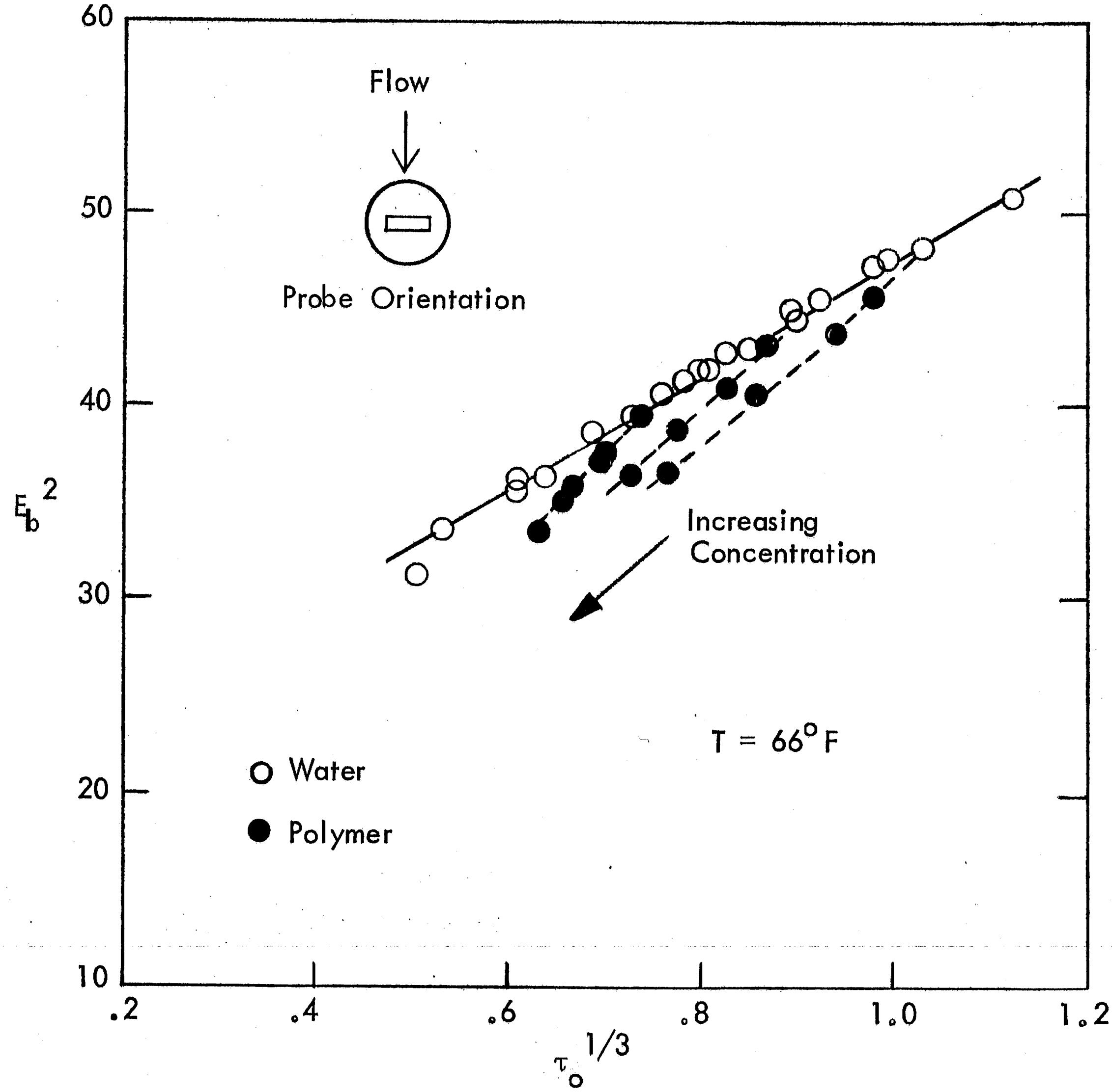

Fig. 5 - Calibration Curve for Flush Mounted Hot Film Sensor, 4 Inch Pipe

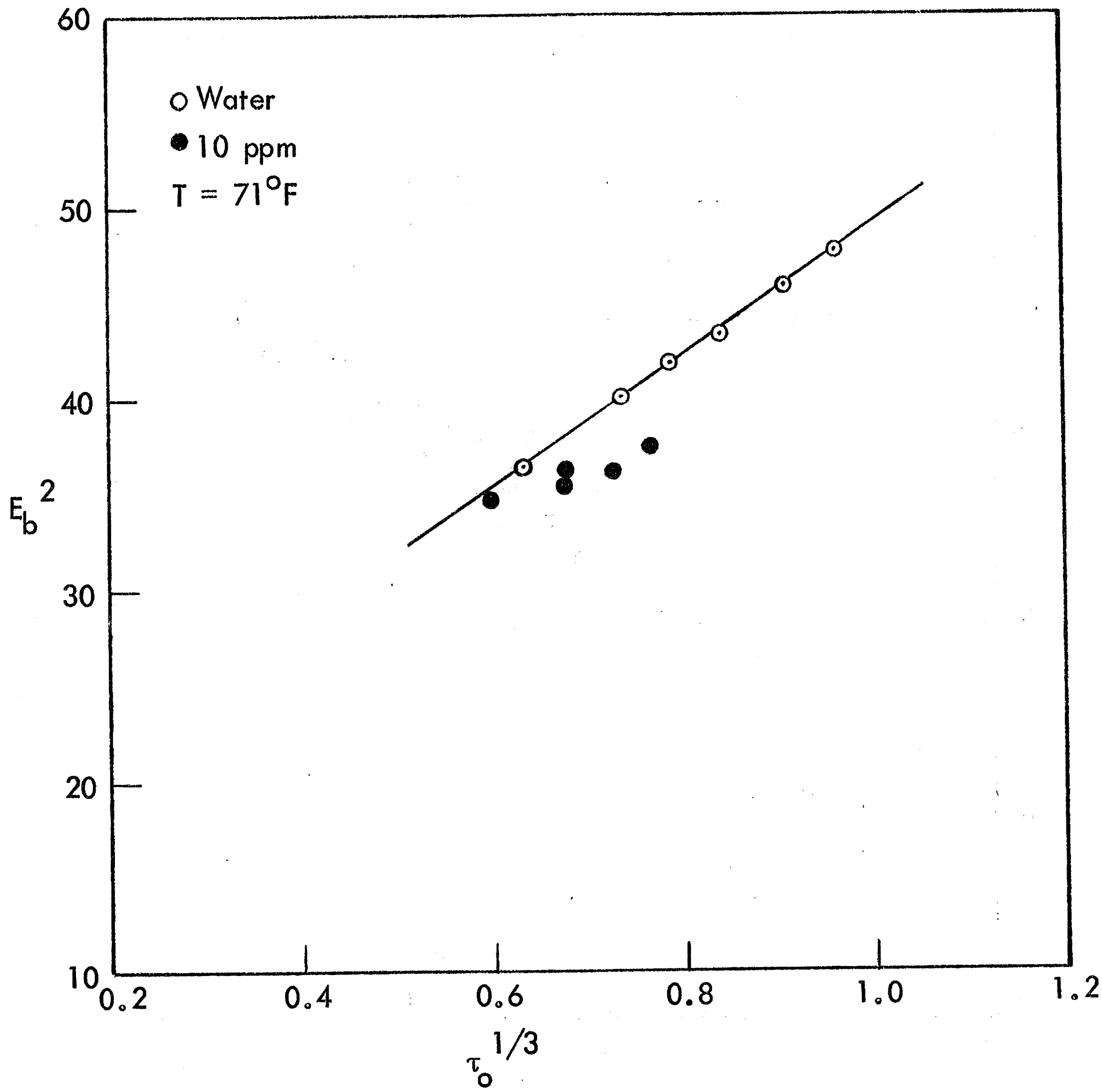

Fig. 6 - Calibration Curves for Flow of Water and Polymer Concentration of 10 ppm, 4 Inch Pipe

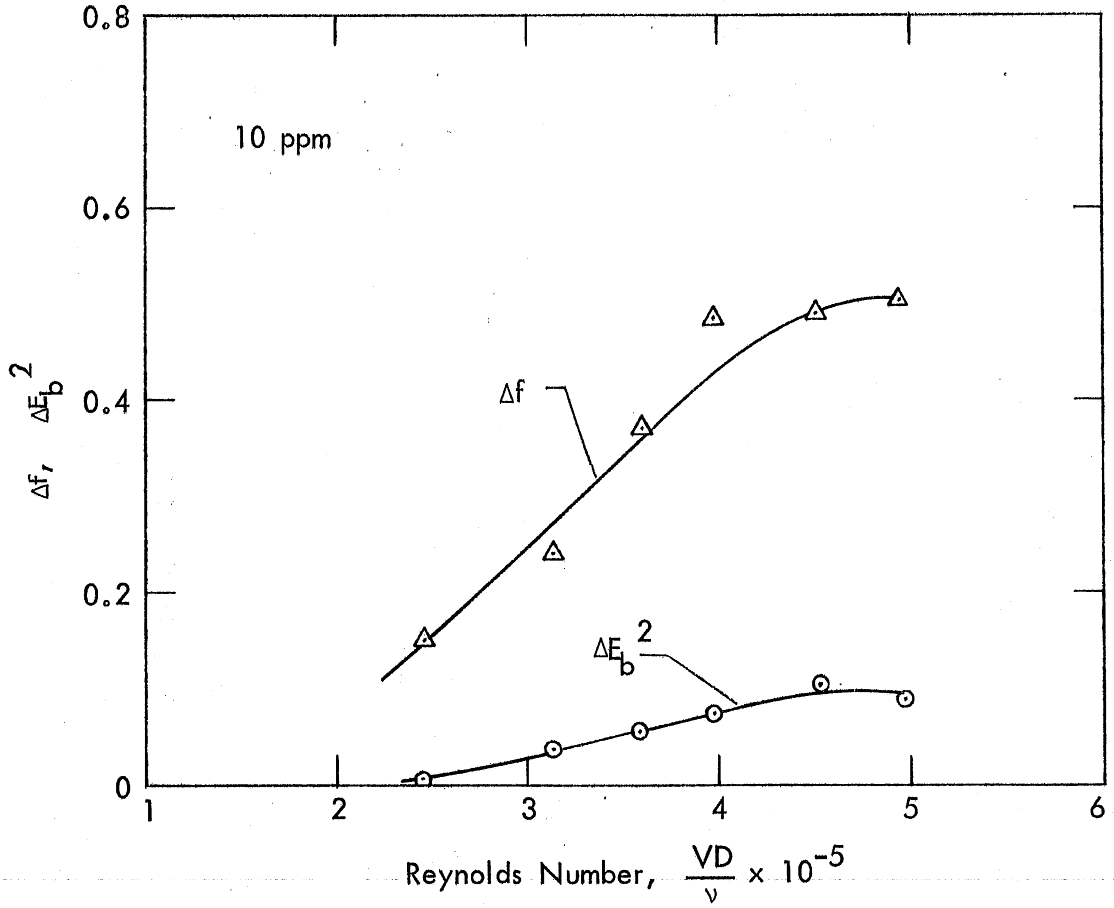

Fig. 7 - Comparison of Friction and Heat Transfer Reductions for Polymer Flow, 4 Inch Pipe

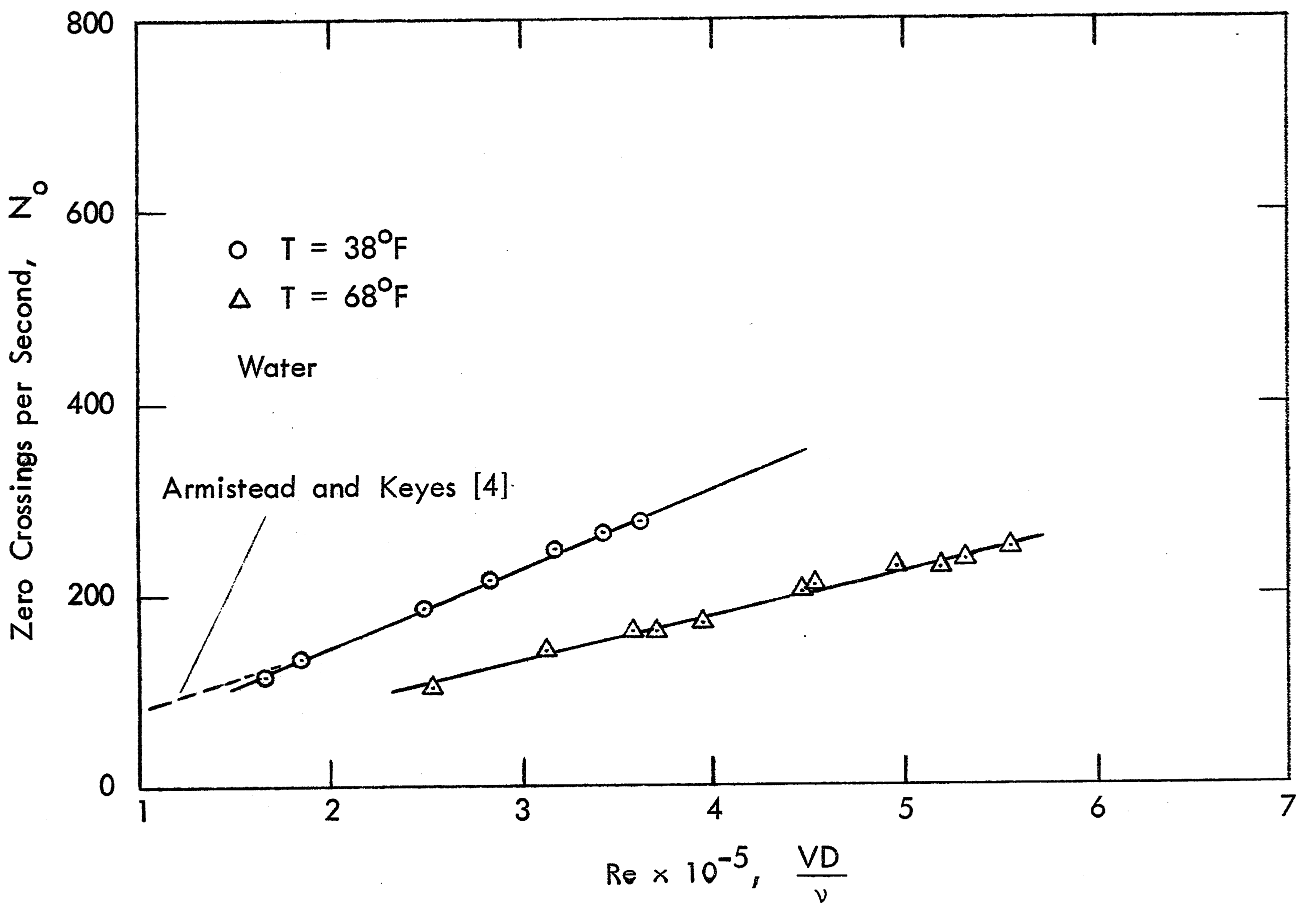

Fig. 8 - Zero Crossing Rate of Heat Transfer Fluctuations as a function of Reynolds Number, 4 Inch Pipe

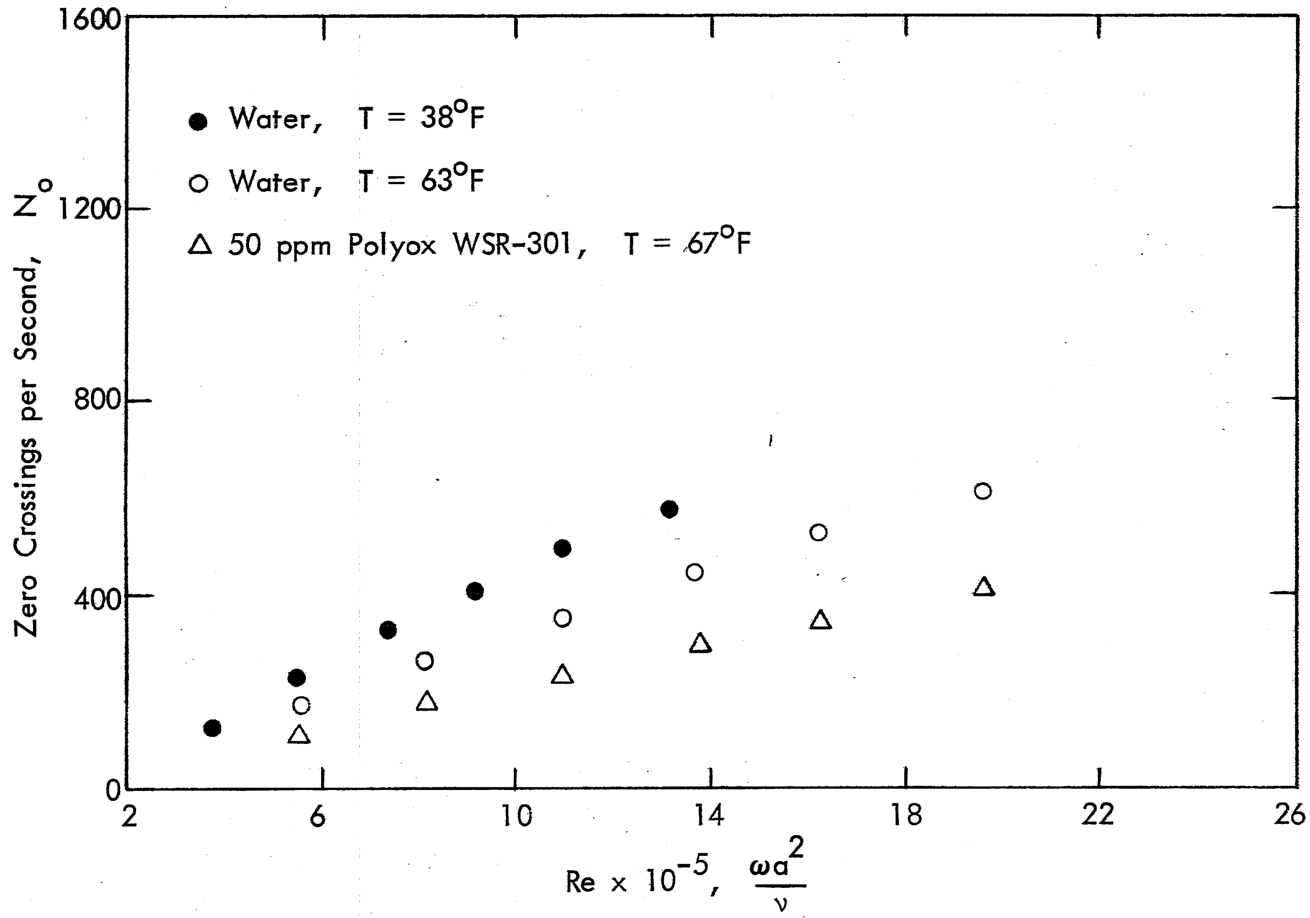

Fig. 9 - Zero Crossing Rate of Heat Transfer Fluctuations as a function of Reynolds Number, Rotating Cylinder

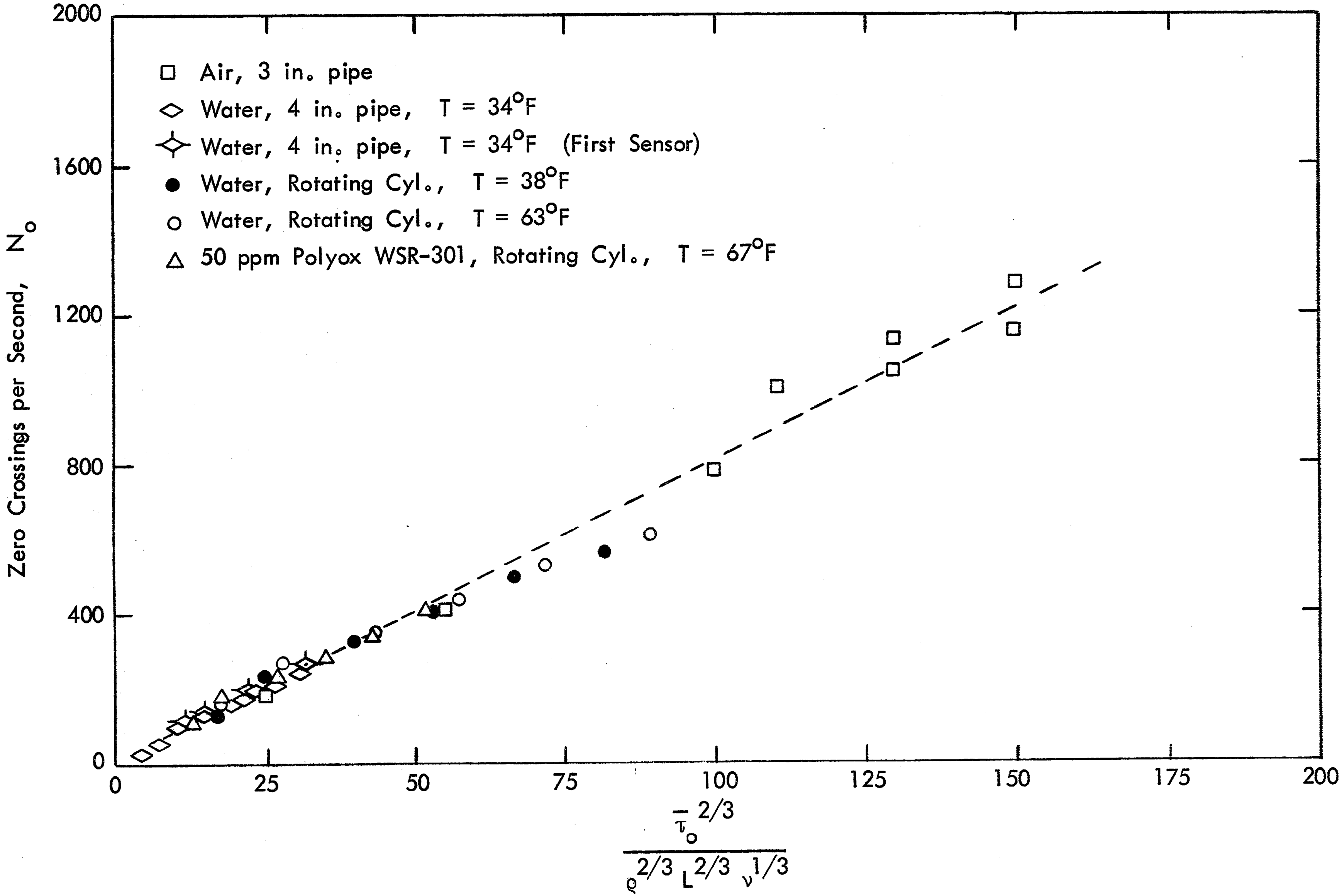

Fig. 10 - Zero Crossing Rate of Heat Transfer Fluctuations as a function of Correlation Parameter for Various Fluids and Flow Facilities

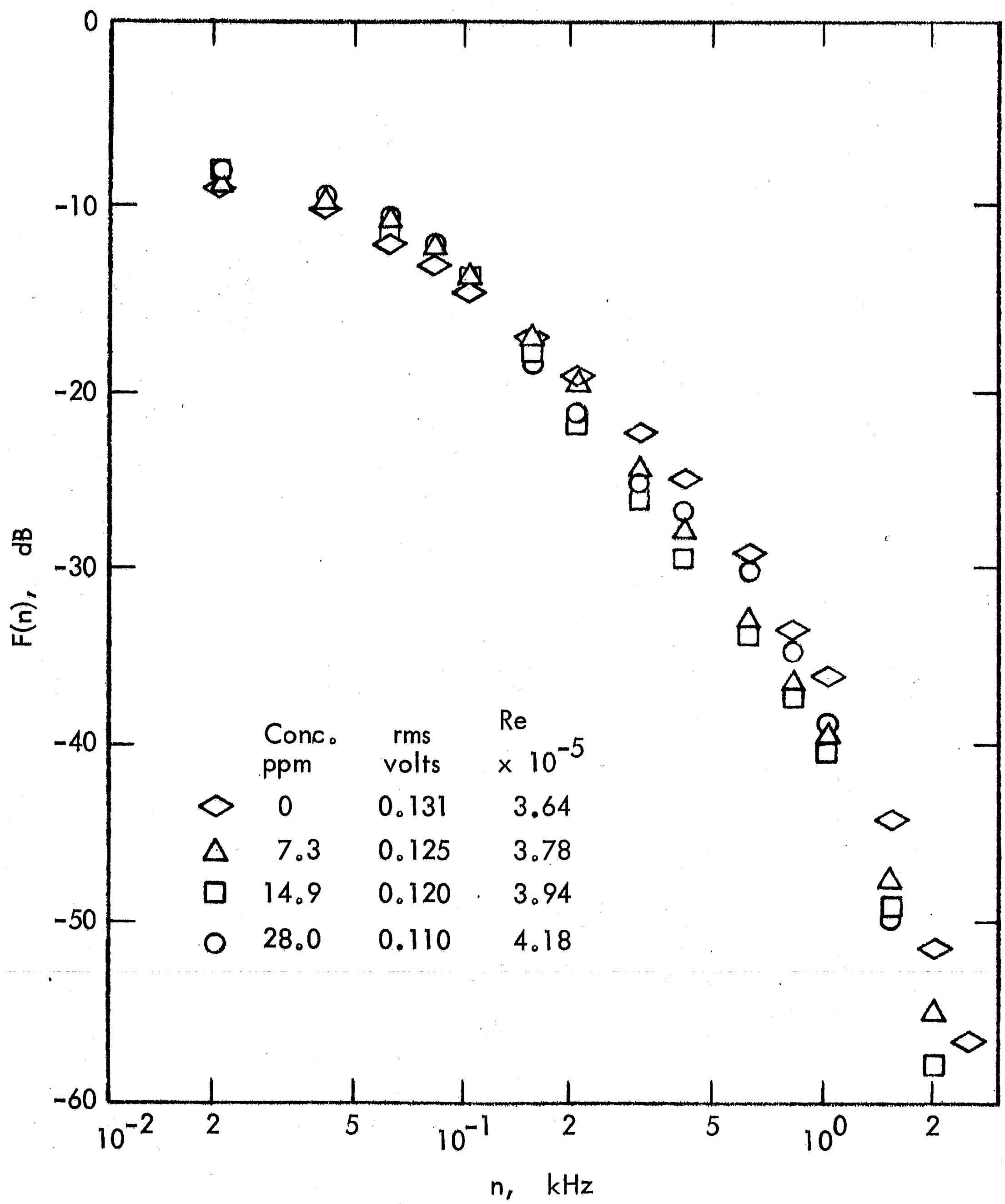

Fig. 11 - Power Spectral Density for Various Polymer Concentrations, 4 Inch Pipe

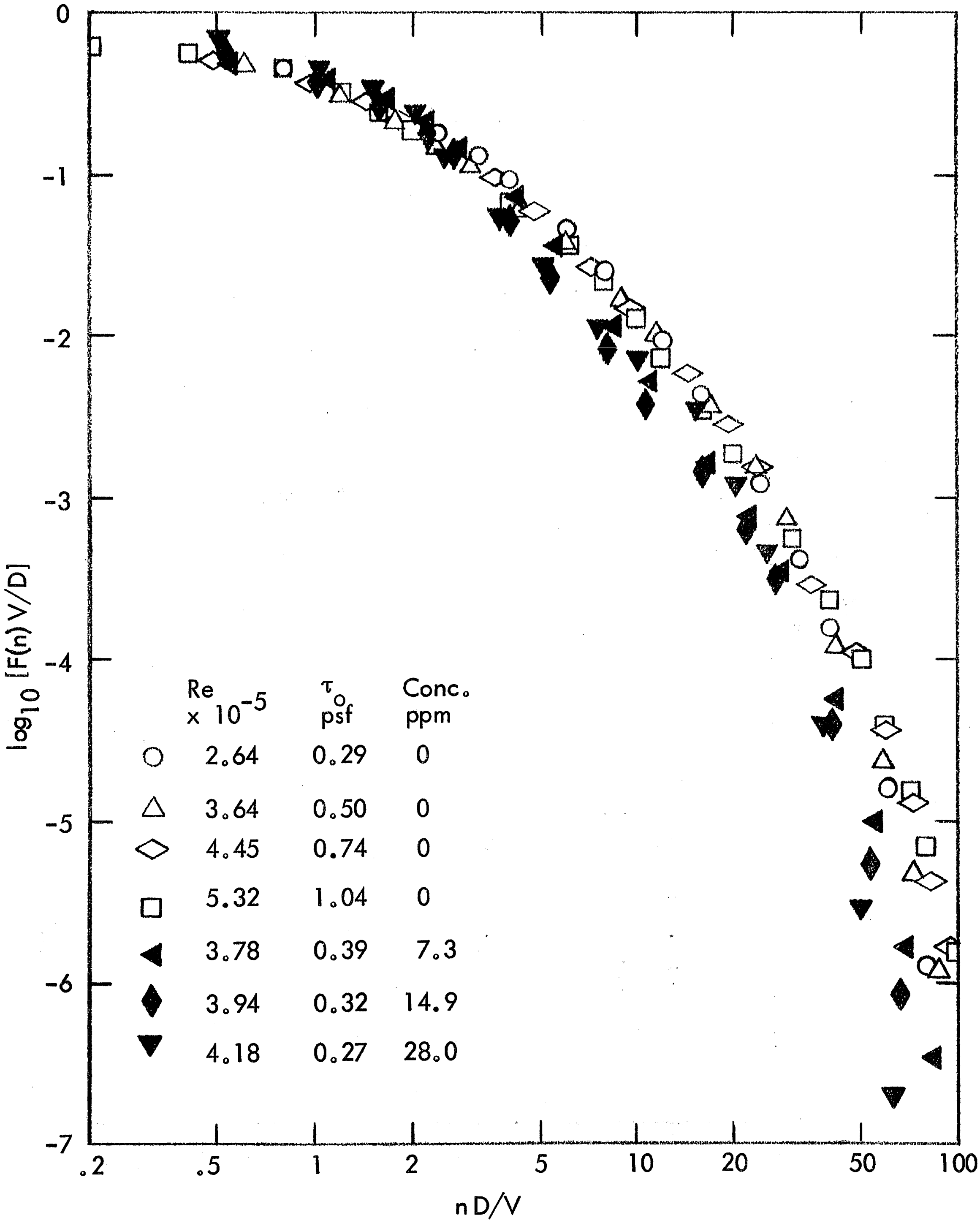

Fig. 12 - Dimensionless Power Spectral Density, 4 Inch Pipe

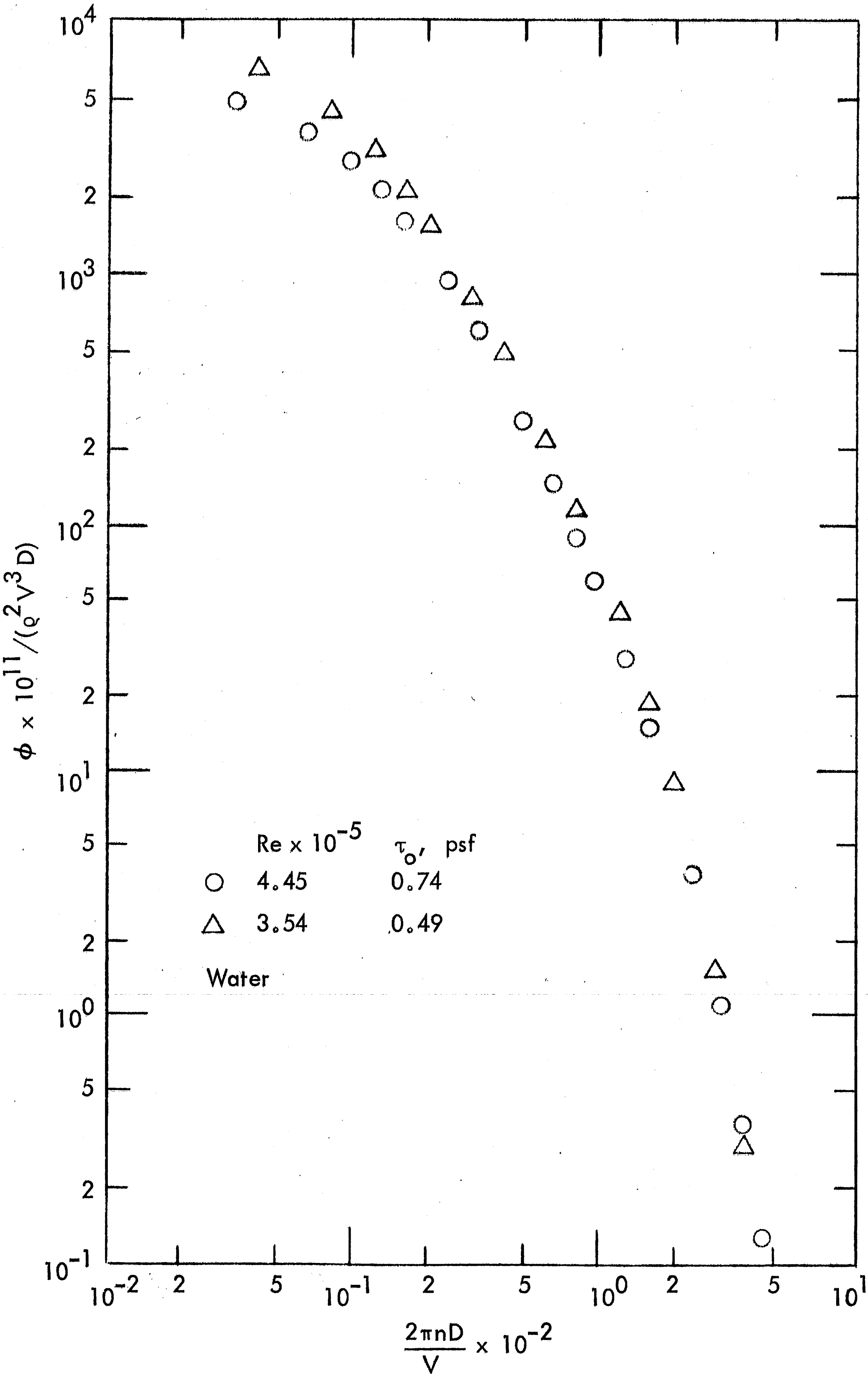

Fig. 13 - Dimensionless Power Spectral Density of Fluctuating Shear Stress, 4 Inch Pipe

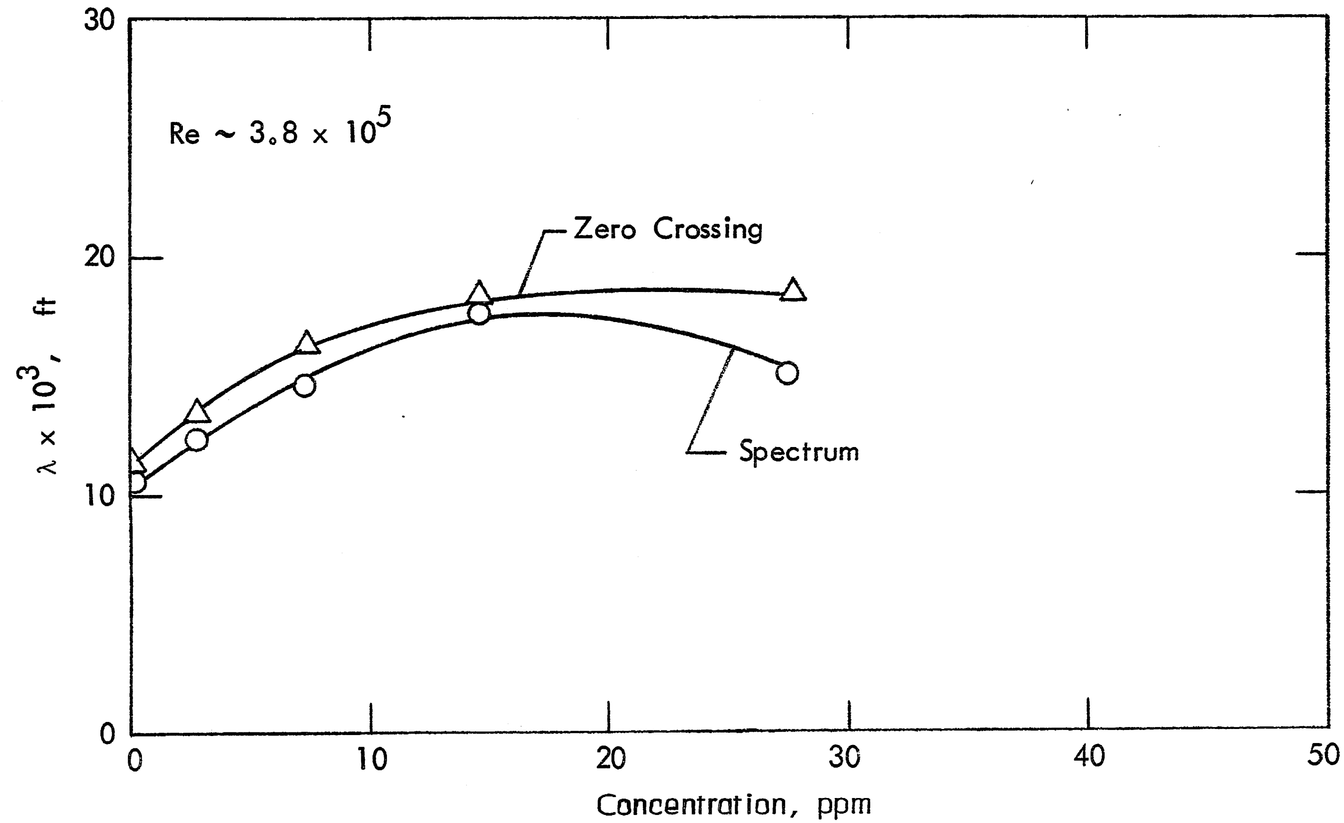

Fig. 14 - Effect of Polymer Additive on Microscale, 4 Inch Pipe

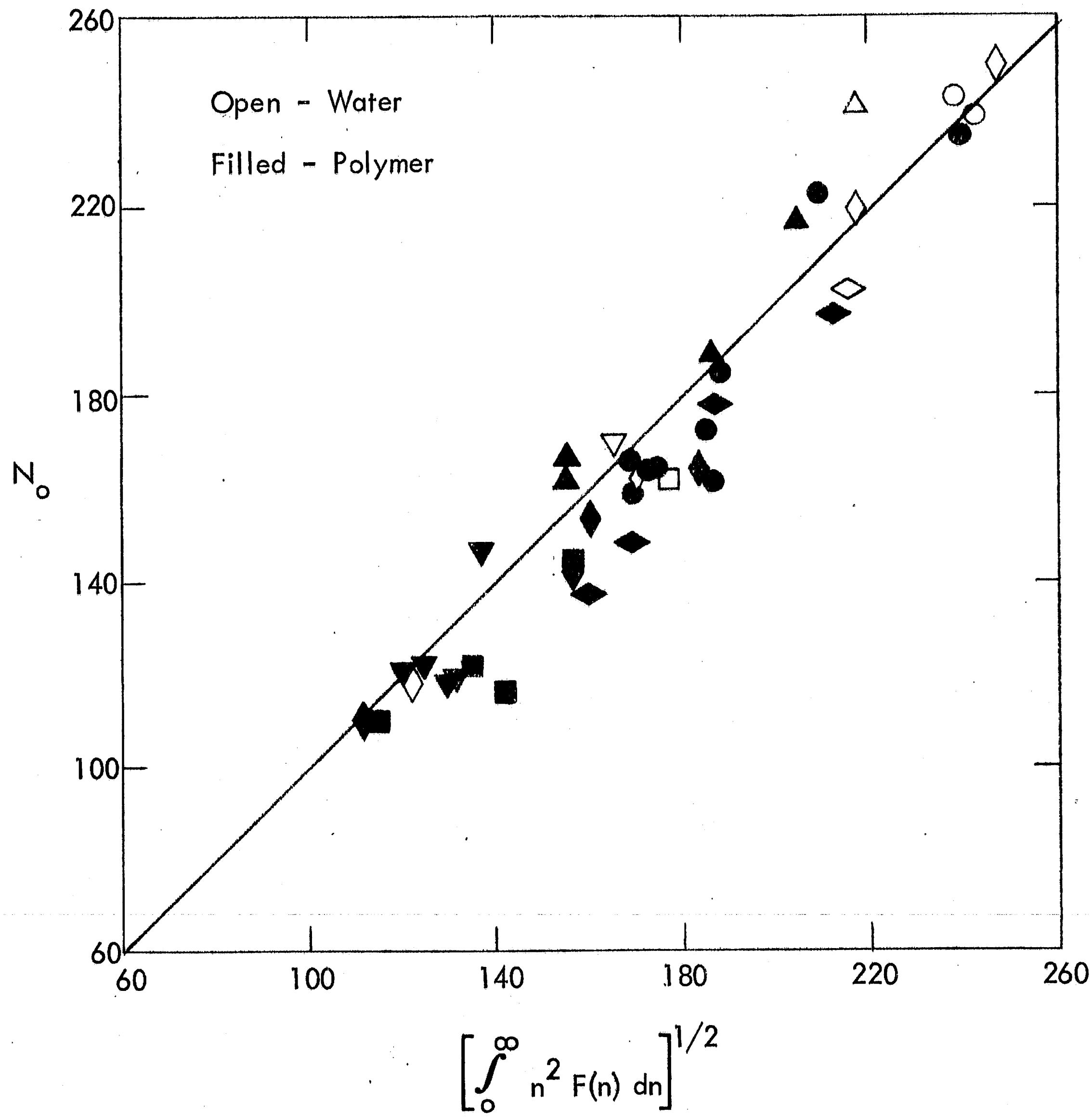

Fig. 15 - Comparison of the Integral of the Second Moment of Frequency Spectra with Zero Crossing Rate, 4 Inch Pipe

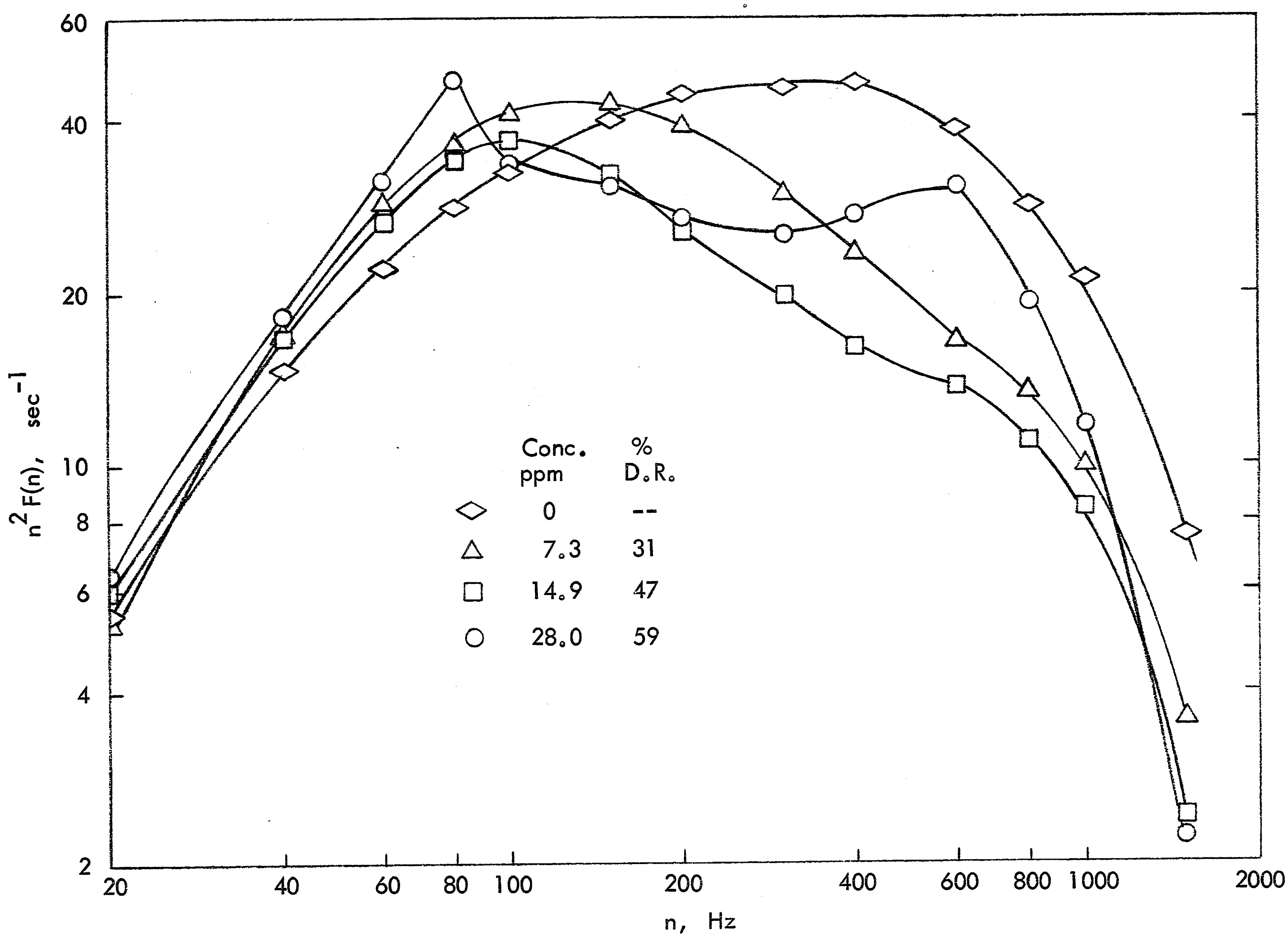

Fig. 16 - Effect of Polymer Additives on Dissipation Spectra, 4 Inch Pipe

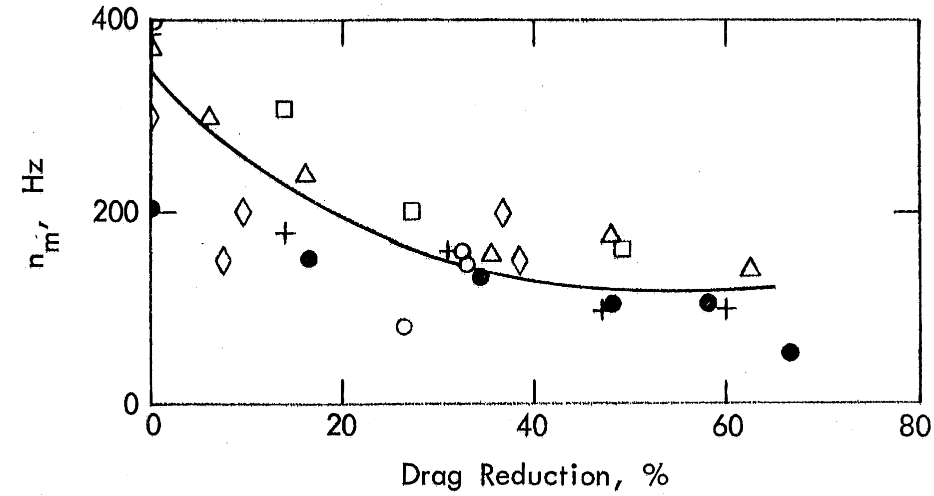

(a)

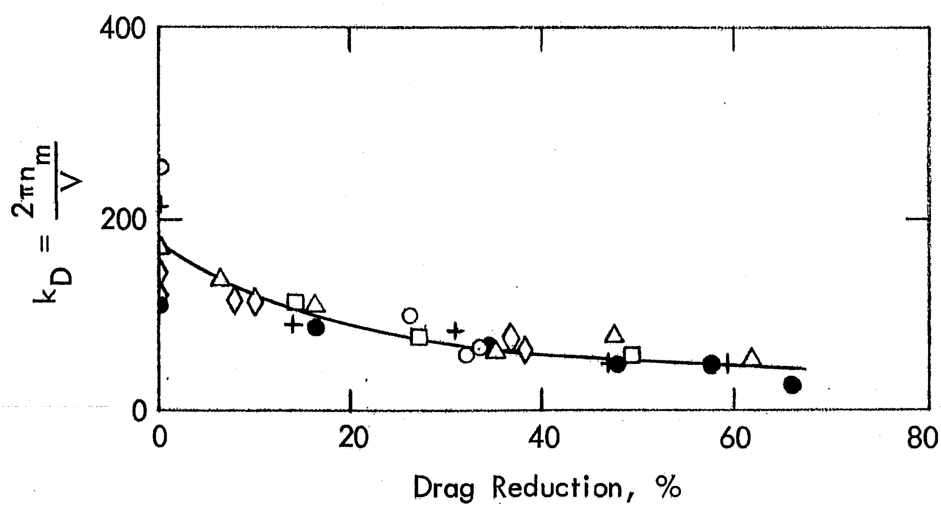

(b)

Fig. 17 - Frequency and Wave Number for Maximum Dissipation as a function of Drag Reduction, 4 Inch Pipe

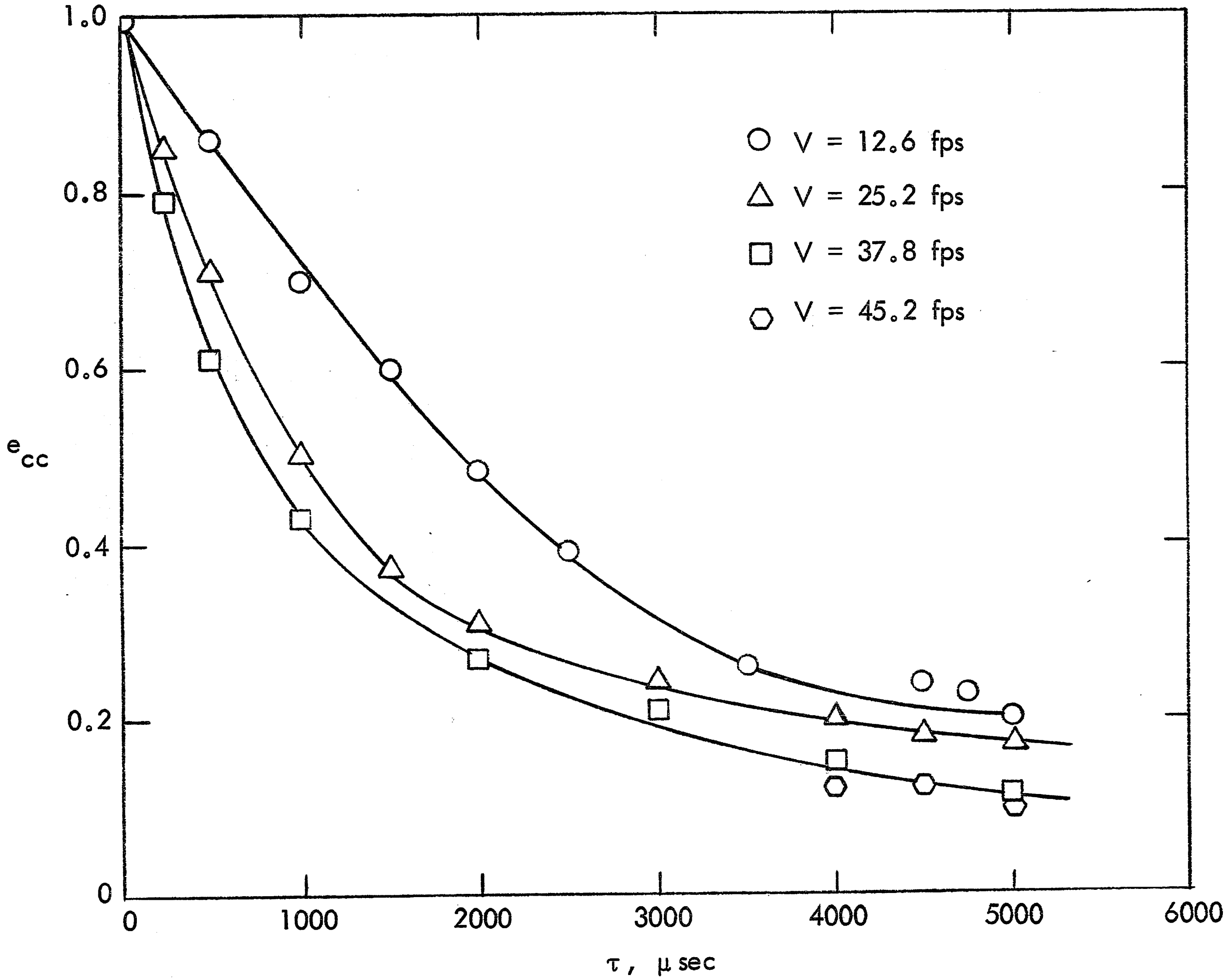

Fig. 18 - Autocorrelation with Hot Film Sensor in Water, Rotating Cylinder

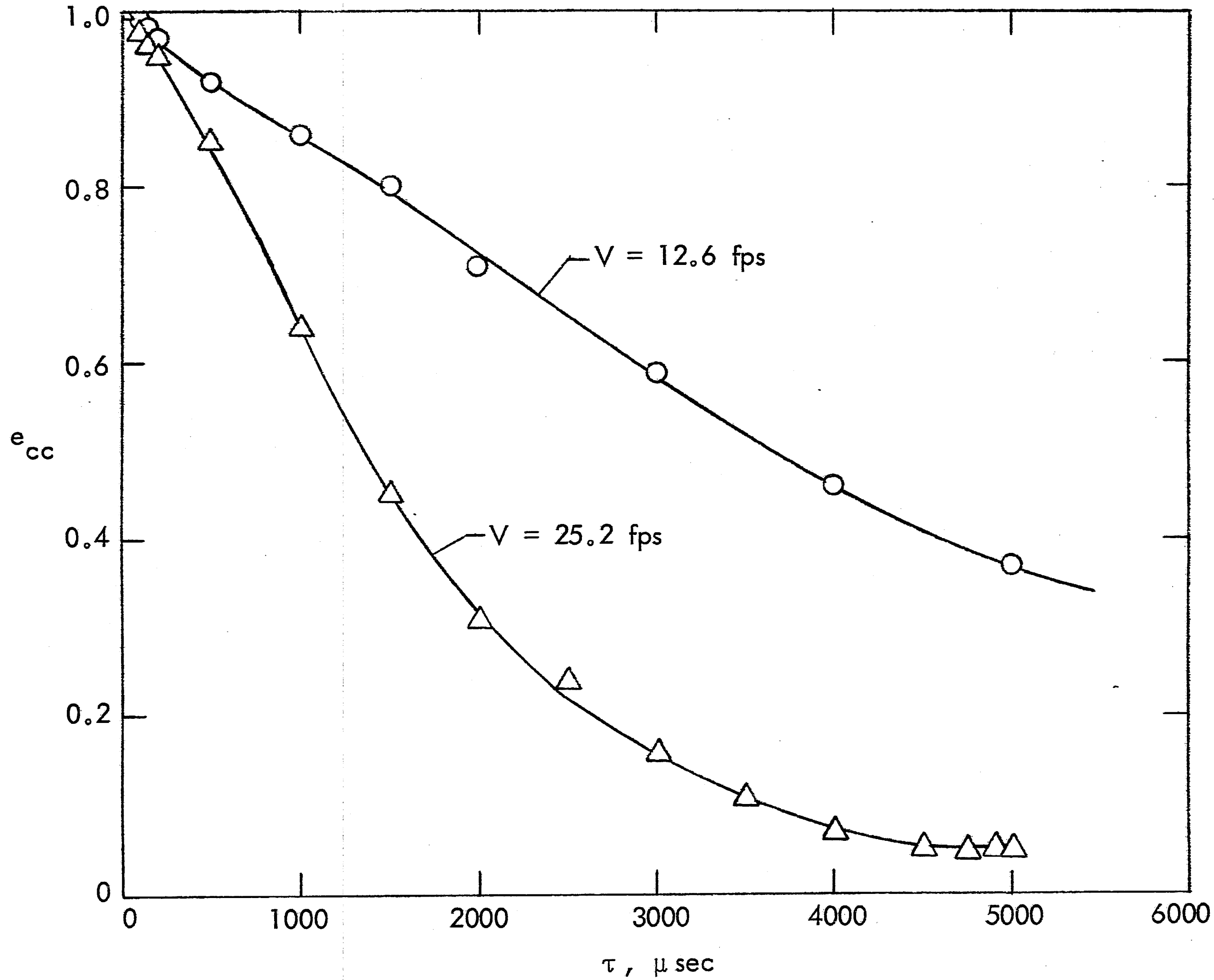

Fig. 19 - Autocorrelation with Hot Film Sensor in 10 ppm Polymer Solution, Rotating Cylinder

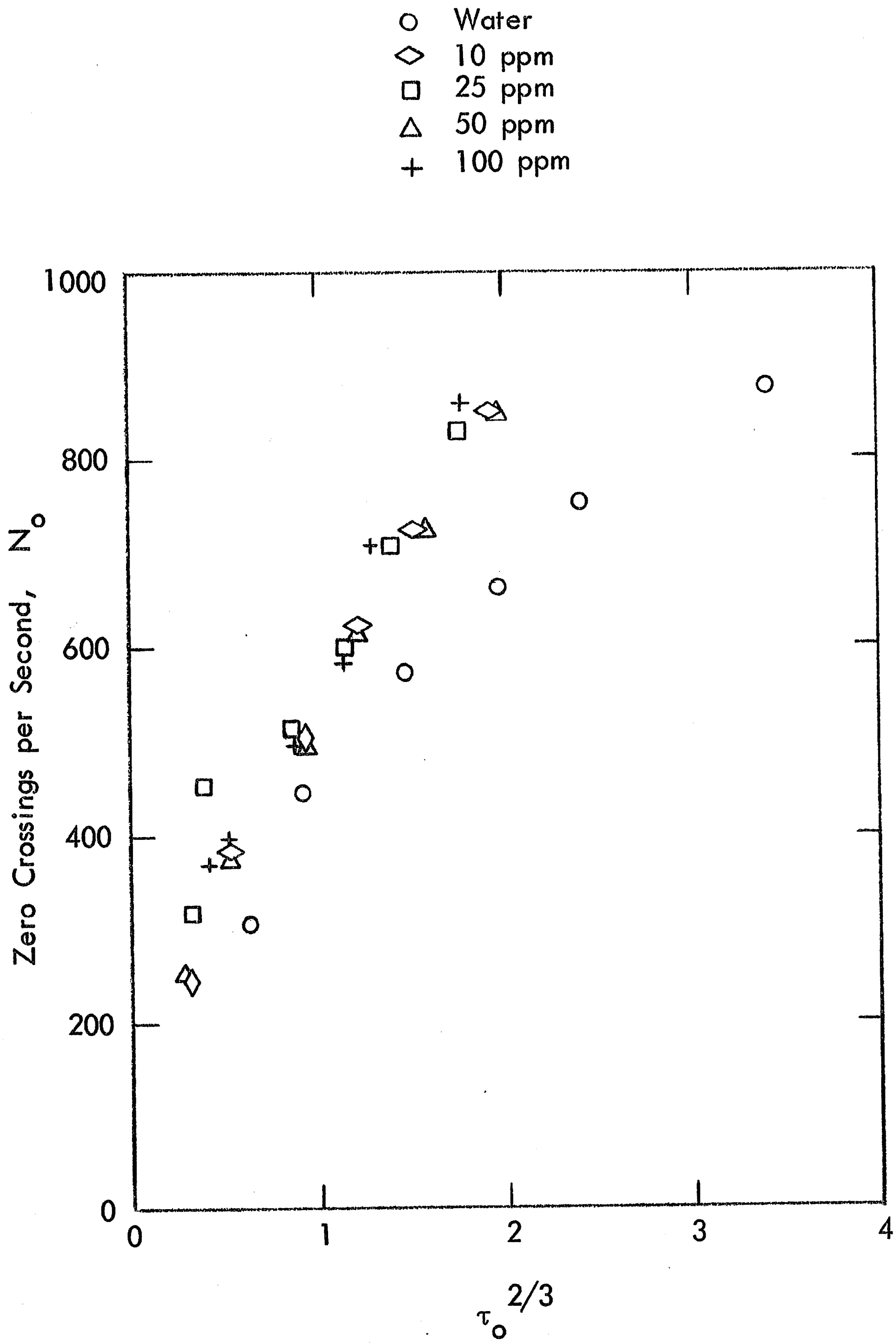

Fig. 20 - Zero Crossing Rate for Surface Pressure Fluctuations, Rotating Cylinder

DISTRIBUTION LIST FOR PROJECT REPORT NO. 134

of the St. Anthony Falls Hydraulic Laboratory

Copies	Organization
40	Commander, Naval Ship Research and Development Center, Bethesda, Maryland 20034, Attn: Code 1505; Code 5614 (39)
1	Officer-in-Charge, Annapolis Laboratory, Naval Ship Research and Development Center, Annapolis, Maryland 21402, Attn: Code 5642 (Library)
6	Commander, Naval Ship Systems Command, Washington, D.C. 20360, Attn: SHIPS 2052 (3); SHIPS 03412B; SHIPS 0372
12	Director, Defense Documentation Center, 5010 Duke Street, Alexandria, Virginia 22314
1	Office of Naval Research, 800 N. Quincy Street, Arlington, Virginia 22217, Attn: Mr. R. D. Cooper (Code 438)
1	Office of Naval Research Branch Office, 492 Summer Street, Boston, Mass. 02210
1	Office of Naval Research Branch Office (493), 536 S. Clark Street, Chicago, Illinois 60605
1	Chief Scientist, Office of Naval Research Branch Office, 1030 E. Green Street, Pasadena, CA 91106
1	Office of Naval Research Resident Representative, 207 West 24th Street, New York, New York 10011
1	Office of Naval Research Resident Representative, 50 Fell Street, San Francisco, CA 94102
2	Director, Naval Research Laboratory, Washington, D.C. 20390, Attn: Code 2027; Code 2629 (ONRL)
1	Commander, Naval Facilities Engineering Command (Code 032C), Washington, D.C. 20390
1	Library of Congress, Science and Technology Division, Washington, D.C. 20540
1	Commander, Naval Ordnance Systems Command (ORD 035), Washington, D.C. 20360
1	Commander, Naval Electronics Laboratory Center (Library), San Diego, CA 92152

Copies

8 Commander, Naval Ship Engineering Center, Center Building, Prince Georges Center, Hyattsville, Maryland 20782, Attn:

SEC 6034B	SEC 6136
SEC 6110	SEC 6144G
SEC 6114H	SEC 6140B
SEC 6120	SEC 6148

1 Library (Code 1640), Naval Oceanographic Office, Washington, D.C. 20390

1 Technical Library, Naval Proving Ground, Dehlgren, Virginia 22448

1 Commander (ADL), Naval Air Development Center, Warminster, Penna 18974

1 Commanding Officer (L31), Naval Civil Engineering Laboratory, Port Hueneme, CA 93043

1 Commander, Naval Undersea Center, San Diego, CA 92132, Attn: Dr. A. Fabula (6005)

2 Officer-in-Charge, Naval Undersea Center, Pasadena, CA 91107, Attn:
Dr. J. Hoyt (2501)
Library (13111)

1 Director, Naval Research Laboratory, Underwater Sound Reference Division, P.O. Box 8337, Orlando, Florida 32806

1 Library, Naval Underwater Systems Center, Newport, R.I. 02840

1 Research Center Library, Waterways Experiment Station, Corps of Engineers, P.O. Box 631, Vicksburg, Mississippi 39180

2 National Bureau of Standards, Washington, D.C. 20234, Attn:
P. Klebanoff (FM 105), Fluid Mechanics
Hydraulic Section

1 AFOSR/NAM, 1400 Wilson Blvd., Arlington, Virginia 22209

1 AFFOL/FYS (J. Olsen), Wright Patterson AFB, Dayton, Ohio 45433

1 Dept. of Transportation, Library TAD-491.1, 400 - 7th Street S.W., Washington, D.C. 20590

1 Boston Naval Shipyard, Planning Dept. Bldg. 39, Technical Library, Code 202.2, Boston, Mass. 02129

1 Charleston Naval Shipyard, Technical Library, Naval Base, Charleston, S. C. 29408

1 Norfolk Naval Shipyard, Technical Library, Portsmouth, Virginia 23709

1 Philadelphia Naval Shipyard, Philadelphia, Penna 19112, Attn: Code 240

Copies

1 Portsmouth Naval Shipyard, Technical Library, Portsmouth, N. H. 03801

1 Puget Sound Naval Shipyard, Engineering Library, Bremerton, Wash. 98314

1 Long Beach Naval Shipyard, Technical Library (246L), Long Beach, CA 90801

1 Hunters Point Naval Shipyard, Technical Library (Code 202.3), San Francisco, CA 94135

1 Pearl Harbor Naval Shipyard, Code 202.32, Box 400, FPO, San Francisco, CA 96610

1 Mare Island Naval Shipyard, Shipyard Technical Library, Code 202.3, Vallejo, CA 94592

1 Assistant Chief Design Engineer for Naval Architecture (Code 250), Mare Island Naval Shipyard, Vallejo, CA 94592

3 U.S. Naval Academy, Annapolis, Maryland 21402, Attn:
Technical Library
Dr. Bruce Johnson
Prof. P. Van Mater, Jr.

3 Naval Postgraduate School, Monterey, CA 93940, Attn:
Library, Code 2124
Dr. T. Sarpkaya
Prof. J. Miller

1 Capt. L. S. McCready, USMS, Director, National Maritime Research Center, U.S. Merchant Marine Academy, Kings Point, L.I., N.Y. 11204

1 U.S. Merchant Marine Academy, Kings Point, L.I., N.Y. 11204, Attn: Academy Library

1 Library, The Pennsylvania State University, Ordnance Research Laboratory, P.O. Box 30, State College, Penna. 16801

1 Bolt, Beranek and Newman, 1501 Wilson Blvd., Arlington, Virginia 22209, Attn: Dr. F. Jackson

1 Bolt, Beranek and Newman, 50 Moulton Street, Cambridge, Mass. 02138, Attn: Library

1 Bethlehem Steel Corporation, Center Technical Division, Sparrows Point Yard, Sparrows Point, Maryland 21219

1 Bethlehem Steel Corporation, 25 Broadway, New York, New York 10004, Attn: Library (Shipbuilding)

1 Cambridge Acoustical Associates, Inc., 1033 Mass Avenue, Cambridge, Mass. 02138, Attn: Dr. M. Junger

Copies

1 Cornell Aeronautical Laboratory, Aerodynamic Research Dept., P.O. Box 235, Buffalo, N.Y. 14221, Attn: Dr. A. Ritter

1 Eastern Research Group, P.O. Box 222, Church Street Station, New York, New York 10008

1 Esso International, Design Division, Tanker Dept., 15 West 51st Street, New York, New York 10019

1 Mr. V. Boatwright, Jr., R and D Manager, Electric Boat Division, General Dynamics Corporation, Groton, Conn. 06340

1 Gibbs and Cox, Inc., Technical Information Control Section, 21 West Street, New York, New York 10006

1 Hydronautics, Inc., Pindell School Road, Howard County, Laurel, Maryland 20810, Attn: Library

2 McDonnell Douglas Aircraft Co., 3855 Lakewood Blvd., Long Beach, CA 90801, Attn:
J. Hess
A.M.O. Smith

1 Lockheed Missiles and Space Co., P.O. Box 504, Sunnyvale, CA 94088, Attn: Mr. R. L. Waid, Dept. 57-74, Bldg. 150, Facility 1

1 Newport News Shipbuilding and Dry Dock Company, 4101 Washington Avenue, Newport News, Virginia 23607, Attn: Technical Library Dept.

1 North American Aviation, Inc., Space and Information Systems Div., 12214 Lakewood Blvd., Downey, CA 90241, Attn: Mr. Ben Ujihara (SL-20)

1 Nielsen Engineering and Research, Inc., 850 Maude Avenue, Mountain View, CA 94040, Attn: Mr. S. B. Spangler

1 Oceanics, Inc., Technical Industrial Park, Plainview, L.I., N.Y. 11803

1 Society of Naval Architects and Marine Engineers, 74 Trinity Place, New York, New York 10006, Attn: Technical Library

1 Sperry Systems Management Division, Sperry Rand Corporation, Great Neck, N.Y. 11020, Attn: Technical Library

1 Stanford Research Institute, Menlo Park, CA 94025, Attn: Library G-021

2 Southwest Research Institute, P.O. Drawer 28510, San Antonio, Texas 78284, Attn:
Applied Mechanics Review
Dr. H. Abramson

1 Tracor, Inc., 6500 Tracor Lane, Austin, Texas 78721

Copies

1 Mr. Robert Taggart, 3930 Walnut Street, Fairfax, Virginia 22030

1 Ocean Engr. Department, Woods Hole Oceanographic Inst., Woods Hole, Mass. 02543

1 Worcester Polytechnic Inst., Alden Research Laboratories, Worcester, Mass. 01609, Attn: Technical Library

1 Applied Physics Laboratory, University of Washington, 1013 N.E. 40th Street, Seattle, Washington 98105, Attn: Technical Library

1 University of Bridgeport, Bridgeport, Conn. 06602, Attn: Dr. E. Uram

1 Cornell University, Graduate School of Aerospace Engr., Ithaca, New York 14850, Attn: Prof. W. R. Sears

4 University of California, Naval Architecture Department, College of Engineering, Berkeley, CA 94720, Attn:
Library
Prof. J. Paulling
Prof. W. Webster
Prof. J. Wehausen

3 California Institute of Technology, Pasadena, CA 91109, Attn:
Aeronautics Library
Dr. T. Y. Wu
Dr. A. J. Acosta

1 Docs/Repts/Trans Section, Scripps Institution of Oceanography Library, University of California, San Diego, P.O. Box 2367, La Jolla, CA 92037

1 Catholic University of America, Washington, D.C. 20017, Attn: Dr. S. Heller, Dept. of Civil and Mech. Engr.

1 Colorado State University, Foothills Campus, Fort Collins, Colorado 80521, Attn: Reading Room, Engr Res Center

1 University of California at San Diego, La Jolla, CA 92038, Attn: Dr. A. T. Ellis, Dept. of Applied Math

1 Florida Atlantic University, Ocean Engineering Department, Boca Raton, Fla. 33432, Attn: Technical Library

2 Harvard University, Pierce Hall, Cambridge, Mass. 02138, Attn:
Prof. G. Carrier
Gordon McKay Library

1 University of Hawaii, Department of Ocean Engineering, 2565 The Mall, Honolulu, Hawaii 96822, Attn: Dr. C. Bretschneider

1 University of Illinois, Urbana, Illinois 61801, Attn: Dr. J. Robertson

Copies

3 Institute of Hydraulic Research, The University of Iowa, Iowa City, Iowa 52240, Attn:
Library
Dr. L. Landweber
Dr. J. Kennedy

1 The Johns Hopkins University, Baltimore, Md 21218, Attn: Prof. O. Phillips, Mechanics Dept.

1 Kansas State University, Engineering Experiment Station, Seaton Hall, Manhattan, Kansas 66502, Attn: Prof. D. Nesmith

1 University of Kansas, Chm. Civil Engr. Dept. Library, Lawrence, Kansas 60644

5 Department of Ocean Engineering, Massachusetts Institute of Technology, Cambridge, Mass. 02139, Attn:
Department Library
Prof. P. Leehey
Prof. P. Mandel
Prof. M. Abkowitz
Dr. J. Newman

1 Parsons Laboratory, Massachusetts Institute of Technology, Cambridge, Mass. 02139, Attn: Prof. A. Ippen

4 St. Anthony Falls Hydraulic Laboratory, University of Minnesota, Mississippi River at 3rd Avenue S.E., Minneapolis, Minnesota 55414, Attn:
Director
Mr. J. Wetzel
Dr. J. Killen
Dr. C. Song.

3 Department of Naval Architecture and Marine Engineering, University of Michigan, Ann Arbor, Michigan 48104, Attn:
Library
Dr. T. F. Ogilvie
Prof. F. Hammitt

2 College of Engineering, University of Notre Dame, Notre Dame, Indiana 46556, Attn:
Engineering Library
Dr. A. Strandhagen

2 New York University, Courant Inst. of Math. Sciences, 251 Mercier Street, New York, New York 10012, Attn:
Prof. A. Peters
Prof. J. Stoker

1 New York University, University Heights, Bronx, New York 10453, Attn: Prof. W. Pierson, Jr.

1 Department of Aerospace and Mechanical Sciences, Princeton University, Princeton, N.J. 08540, Attn: Prof. G. Mellor

Copies

3 Davidson Laboratory, Stevens Institute of Technology, 711 Hudson Street, Hoboken, New Jersey 07030, Attn:
Library
Mr. J. Breslin
Mr. S. Tsakonas

1 Department of Mathematics, St. John's University, Jamaica, New York 11432, Attn: Prof. J. Lurye

1 Applied Research Laboratory Library, University of Texas, P.O. Box 8029, Austin, Texas 78712

1 College of Engineering, Utah State University, Logan, Utah 84321, Attn: Dr. R. Jeppson

2 Stanford University, Stanford, CA 94305, Attn:
Engineering Library
Dr. R. Street

3 Webb Institute of Naval Architecture, Crescent Beach Road, Glen Cover, L.I., N.Y. 11542, Attn:
Library
Prof. E. V. Lewis
Prof. L. W. Ward

1 National Science Foundation, Engineering Division Library, 1800 G Street N.W., Washington, D.C. 20550

1 University of Connecticut, Box U-37, Storrs, Conn. 06268, Attn: Dr. V. Scottron, Hydraulic Research Lab

1 Long Island University, Graduate Department of Marine Science, 40 Merrick Avenue, East Meadow, L.I., N.Y. 11554, Attn: Prof. David Price

1 Dr. Douglas E. Humphreys (Code 712), Naval Coastal Systems Laboratory, Panama City, Florida 32401

Unclassified

Security Classification

DOCUMENT CONTROL DATA - R & D

(Security classification of title, body of abstract and indexing annotation must be entered when the overall report is classified)

1. ORIGINATING ACTIVITY (Corporate author) St. Anthony Falls Hydraulic Laboratory University of Minnesota	2a. REPORT SECURITY CLASSIFICATION Unclassified 2b. GROUP

3. REPORT TITLE

A PRELIMINARY REPORT ON THE ZERO-CROSSING-RATE TECHNIQUE FOR AVERAGE SHEAR MEASUREMENT IN FLOWING FLUID

4. DESCRIPTIVE NOTES (Type of report and, inclusive dates)

Project Report - October 1968 - April 1970

5. AUTHOR(S) (First name, middle initial, last name)

Joseph M. Wetzel
John M. Killen

6. REPORT DATE November 1972	7a. TOTAL NO. OF PAGES 38	7b. NO. OF REFS 14
8a. CONTRACT OR GRANT NO. N00014-67-A-0113-0007 and N00014-67-A-0113-0015 b. PROJECT NO. c. d.	9a. ORIGINATOR'S REPORT NUMBER(S) Project Report No. 134 9b. OTHER REPORT NO(S) (Any other numbers that may be assigned this report)	

10. DISTRIBUTION STATEMENT

Approved for public release; distribution unlimited

11. SUPPLEMENTARY NOTES	12. SPONSORING MILITARY ACTIVITY Naval Ship Research and Development Center, Bethesda, Maryland 20034

13. ABSTRACT

The characteristics of a flush-mounted hot film sensor were investigated in turbulent flows of both water and drag reducing polymer solutions in a 4-inch-diameter pipe. For water flows, a linear relationship was found between the average power supplied to the sensor and the cube root of the wall shear stress. With the addition of polymer additives, the heat transfer rates at a given shear stress were reduced from those found with water alone. Analysis of the heat transfer fluctuations occurring in various flow facilities has shown that the zero crossing rate is related to the wall shear stress and to fluid properties for water, polymer, and air flows. The zero crossing rate is not dependent on hot film sensitivity or contamination. Evaluations of the fluctuation microscale indicated that it had been increased by the addition of drag reducing polymer to the water. Autocorrelation measurements were made of the heat transfer fluctuations, but the limited data for the autocorrelations were not conclusive. Attempts to obtain cross-correlation coefficients between heat transfer and surface pressure fluctuations as measured with a small hydrophone were unsuccessful. The zero crossing rate of the surface pressure fluctuations was found to be related to the local wall shear stress.

DD FORM 1 NOV 65 1473 (PAGE 1)

Unclassified

Security Classification

Unclassified
Security Classification

14. KEY WORDS	LINK A		LINK B		LINK C	
	ROLE	WT	ROLE	WT	ROLE	WT
Drag reduction						
Polymer additives						
Turbulence						